DANMARKS OG GRØNLANDS GEOLOGISKE UNDERSØGELSE RAPPORT 2004/104

Source rocks for SW Indian heavy sand deposits

A study of ilmenite alteration patterns and ilmenite and garnet chemistry of potential source rocks for high-Ti ilmenite in beach sediments

Stefan Bernstein

GEOLOGICAL SURVEY OF DENMARK AND GREENLAND
MINISTRY OF THE ENVIRONMENT

G E U S

DANMARKS OG GRØNLANDS GEOLOGISKE UNDERSØGELSE RAPPORT 2004/104

Source rocks for SW Indian heavy sand deposits

A study of ilmenite alteration patterns and ilmenite and garnet chemistry of potential source rocks for high-Ti ilmenite in beach sediments

Stefan Bernstein

Released 25.11.2009

GEOLOGICAL SURVEY OF DENMARK AND GREENLAND
MINISTRY OF THE ENVIRONMENT

GEUS

Contents

1. Abstract

A detailed electron-microprobe study of ilmenite and garnet from basement rocks in SW India reveals that:

- The source rocks for high Ti ilmenite deposits along the SW Indian beaches are sillimanite- and garnet bearing, orthopyroxene-free paragneisses, which are characterized by having garnets with low grossular components (<5%) and low MnO contents (<0.6 wt. %).
- Ilmenite from nearly all the basement rocks shows incipient alteration to pseudo-rutile.
- The style of ilmenite alteration correlates with rock type, i. e. the rocks identified as potential source rocks for the high Ti ilmenite in the sediments, show the most intense alteration.
- Because sediments from rivers show only modest contents of altered ilmenite, this *in situ* alteration of ilmenite is not the process responsible for the Ti enrichment in ilmenite from beach deposits, but it shows that the ilmenite from the paragneisses are prone to alteration.
- It is found that apatite often form impurities in the pseudo-rutile, with concentrations up to 0.7 wt. % P_2O_5. Apatite is thus formed very early in the alteration process.

Recommendations for future research:

- Detail electron-microprobe study of altered ilmenite and garnet from beach sediments, in order to characterize the type of alteration and alteration products, and to address the issue of phosphate formation in altered ilmenite.
- Trace element analysis with laser ablation ICPMS of altered and unaltered ilmenite and of garnets from beach sediments and from rocks to place tighter constraints on the source of the ilmenite and the place and time of ilmenite alteration.
- Thorough petrogenetic characterization of source rock
- Developing an algorithm for estimating Ti content in ilmenite from whole-rock XRF analysis.

2. Extended summary

High Ti ilmenite is found in beach sediments along the southern part of the Kerala State coast line. Earlier studies (e. g. Bernstein, 2003) have suggested that the source for the ilmenite with elevated Ti contents is found within the high grade metasediments of the Kerala khondalite belt. In order to place some tighter constraints on this hypothesis, garnet and ilmenite from a series of rock samples, taken from throughout the Kerala State, were analysed by electron microprobe. The rock samples largely belongs to two distinct groups. 1) a diorite-granite-charnockite group, dominating the middle and northern part of Kerala State, and which rarely contain garnet. 2) the Kerala Khondalite Belt, occupying the southern portion of the Kerala and Tamil Nadu states. The khondalite belt contains some charnockites, but is characterised by abundant high grade metamorphic sediments, rich in garnet.
Ilmenite from the rock samples display large variations in chemistry, but in general those from khondalite lithologies have elevated TiO_2 contents (>50 wt.% TiO_2), whereas most of the rock samples from outside the khondalite belt, have TiO_2 contents below 50 wt. %. Ilmenite from garnet-free lithologies tend to have high MnO (>1 wt. %), while low MnO (<0.5 wt.%) is typical of samples from the khondalite lithologies. It is, however, difficult from the ilmenite composition alone to put tighter constraints on the possible source rocks for the high Ti ilmenite found in the beach deposits.
The most valuable information on the possible source for the high Ti ilmenite from the beach sediments, comes from garnet compositions. Garnets from these sediments show uniformly low grossular components (< 5%) and low MnO contents (0.4-0.7 wt. %). These are features that they share with garnets from rock samples of the sillimanite-bearing schists of the khondalite belt, and which are distinctly different from high MnO, high grossular garnets from other lithologies from the khondalite belt, and which are further characterised by also containing orthopyroxene. It is unknown why beach sediments with high Ti ilmenite contains overwhelming quantities of garnets from the sillimanite-bearing rocks, but one possible explanation could be that the sillimanite-bearing rocks are more suseptible to erosion and weathering, and thus makes up higher proportions of the sediments in the adjacent sediemntary basins. Also, the sillimanite-bearing rocks tend to have higher modal abundances of both ilmenite and garnet, compared to orthopyroxene lithologies.

Ilmenite grains showing incipient alteration are found in one sample from the diorite-granite-charnockite suite and in several samples from the khondalite belt. The alteration has been studied in detail by electron microprobe traverses across the alteration fronts. It is found that the alteration progresses along a path of oxydation and hydrooxylation of iron, with subsequent leaching of Fe and Mn. The result is the formation of pseudo-rutile or hydroxy pseudorutile with Ti# (=100xTi/(Ti+Fe)) of up to 97. Alteration of ilmenite in the one sample from the diorite-granite-charnockite suite is not as intense as in samples from the khondalite belt, and the altered material has a Ti# of about 60. Typical for most of the altered ilmenite grains is an increase in Si, Al, Mg, Ca, and P along with the decrease in Fe and increase in Ti. This is interpreted as introduction of impurities of silicates, mainly clay minerals. Further leaching to high Ti# usually is followed by a decrease in these elements, which suggests that some of the impurities are leached away during progressive alteration and perhaps recrystallization of Ti rich phases. In many altered grains, P_2O_5 shows a 1:1 correlation with CaO. This is taken to reflect crystallization of apatite in the porous pseudorutile material. With progressive leaching, P_2O_5 and CaO stays at a constant level in contrast to the Al, Si and Mg which reside in silicate impurities. Therefore apatite appears to be resistant to further leaching. The level of P_2O_5 in the ilmenite alteration products is up to about 0.7 wt. %.

Ilmenite alteration is found to occur along grain surfaces and grain edges, and very often along fractures in the ilmenite. This latter finding points towards low temperature conditions, probably at environments close to outcrop surfaces (meters or tens of meters), rather than conditions at elevated temperatures, e. g. at retrograde metamorphism.

3. Introduction

A series of samples from beach and river sediments, and of rocks from the hinterland were collected in 2002 and 2003. The samples were collected from the west and east coasts of Kerala State and from the southeast coast of Tamil Nadu state (Fig. 1). In total, 67 samples were collected in 2002, of which 45 samples represent sediments and 22 represent rocks. In 2003, another 61 sediment samples were collected from the Chavara deposit in SW Kerala State. The results of the CCSEM analyses of the sediment samples were reported in Stendal et al. (2003) and Bernstein (2003). In this report we focus on the chemistry of key minerals from the 22 rock samples, namely ilmenite and garnet, partly to test some of the hypotheses forewarded in Bernstein (2003) and partly to gain additional information on the leaching processes of ilmenite.

Some of the rock samples were also studied by Mads S. Christiansen as part of his masters thesis, but he encountered severe problems with regard to the number of ilmenite grains to be analysed, since many thin sections appeared to contain very few if any ilmenite grains. To circumvent this problem, heavy mineral separates were prepared of each rock sample, as it was hoped that this procedure would concentrate the number of ilmenite grains available for analyses in each sample.

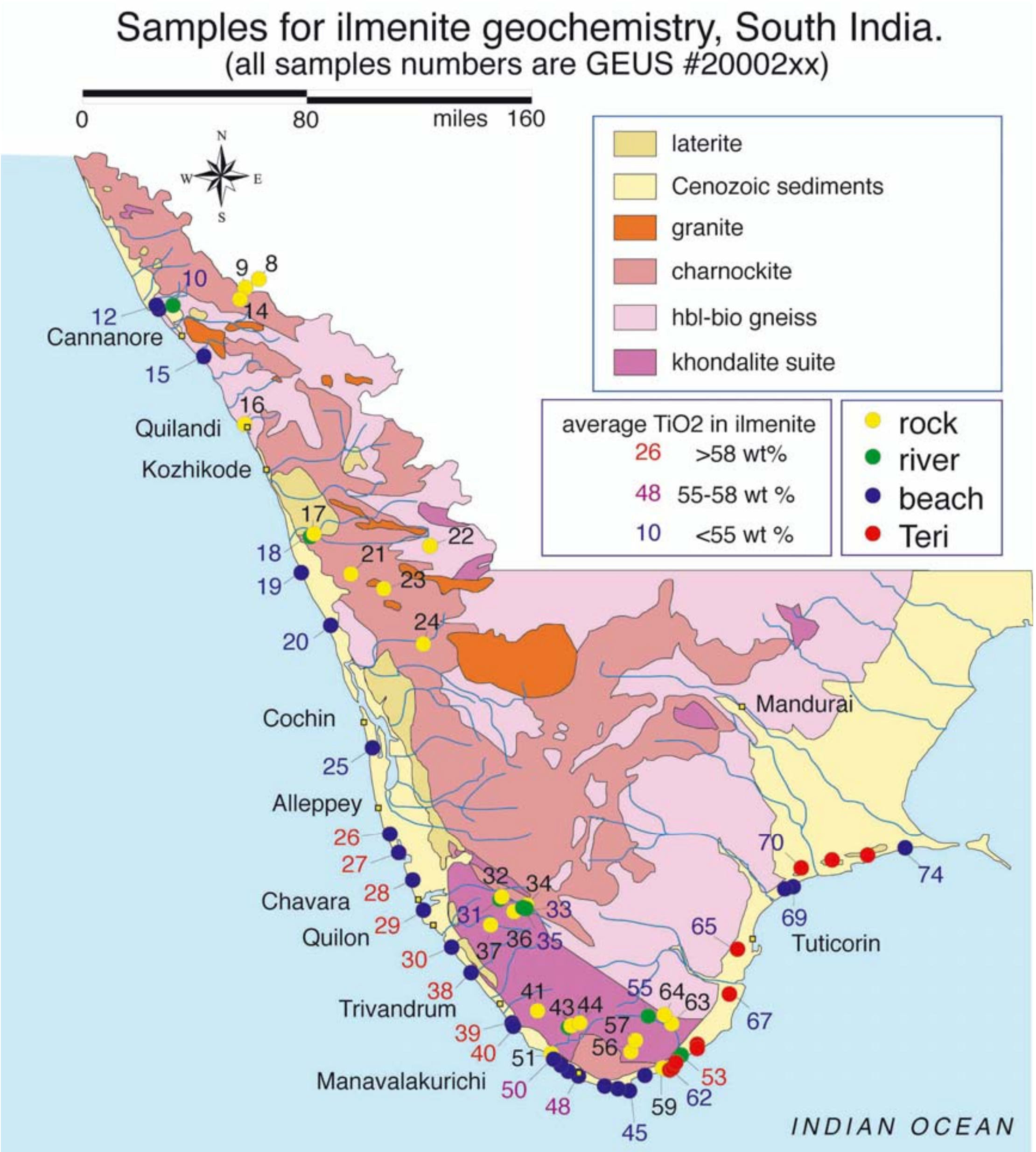

Figure 1. *Map of southern India, including Kerala and southern part of Tamil Nadu states. Circles give sample locations as reported by Stendal et al., 2003 and Bernstein, 2003. Blue, green and red circles represent beach, river and Teri (eolian) sediments. Rock samples, which are the subject of this report, are marked by yellow circles. The colour of the sample number for the sediment samples indicates level of TiO_2 in average ilmenite (see legend).*

4. Sample preparation

The rock samples were crushed by hydraulic jaw-crusher and subsequently in a tungsten-carbide mortar. The size fraction 100-300 μm was then washed and rinsed with millipore H_2O in ultrasonic bath and dried at temperatures of less than 50°C. The grains heavier than 2.8 g/cm^3 were then separated using heavy liquid, mounted in epoxy as a standard thin section and polished. The thin sections are 200 μm thick.

4.1 Analytical procedure

The thin section mounted grains were analysed using the electron microprobe at the Geological Institute, University of Copenhagen. The following elements were measured by the wave dispersive system (peak counting time in seconds given in paranthesis): Al (60), Si (40), Mn (40), Fe (10), Cr (50), Ca (20), Ti (40), Nb (40), P (100), Mg (100). Background and peak positions were measured for the same amount of time. ZAF correction was applied using the JEOL routine system, and both natural and synthetic standards were monitored to assure reproducibility. Both garnet and ilmenite grains were analysed.

5. Results

5.1 Rock samples from Kerala State

The 22 rock samples cover a wide range of lithologies, but can roughly be divided into two main groups. These are the diorite-granitic-charnockite gneisses of the northern region (samples 2000208-224), and the quatzo-felspathic gneisses of the southern region (samples 2000232-264) which all come from the Kerala khondalite belt (Table 1). A few of the samples from the khondalite belt are also orthopyroxene bearing, namely 2000241, 256, 257 and 259, but the khondalite belt samples are otherwise characterized by containing high amounts of garnet (often >10 %) and often sillimanite and relatively high amounts of opaque phases. A short petrographic description of the individual samples is presented in appendix 1, and average compositions for ilmenite and garnet are found in appendix 2.

Table 1. *List of rock samples from Kerala State, SW India*

GEUS sample no.	Field#	region	Lithology
2000208	K1	d-c	Charnockite
2000209	K2	d-c	Garnet-clinopyroxene gneiss
2000214	K7	d-c	Diorite geniss
2000216	K10	d-c	Hornblende-biotite geniss
2000217	K11	d-c	Hornblende dioritic gneiss (charnockite)
2000221	K16	d-c	Hornblende dioritic gneiss
2000222	K19	d-c	Hornblende dioritic gneiss
2000223	K20	d-c	Two-pyroxene gabbroic gneiss
2000224	K23	d-c	Granodioritic gneiss
2000232	K31	k	Garnetiferous quatzo-felspathic gneiss
2000234	K33	k	Garnetiferous quatzo-felspathic gneiss
2000236	K36	k	Garnetiferous quatzo-felspathic gneiss
2000237	K37	k	Garnetiferous diorite
2000241	K41	k	Garnet-orthopyroxene gneiss
2000243	K43	k	Garnetiferous granite
2000244	K44	k	Garnet-bearing granodioritic gneiss
2000251	K51	k	Garnet-bearing granodiorite
2000256	K56	k	Garnet-orthopyroxene gneiss
2000257	K57	k	Garnet-orthopyroxene gneiss
2000259	K61	k	Two-pyroxene gneiss
2000263	K66	k	Garnet-bearing granodioritic gneiss
2000264	K67	k	Garnet-bearing granodioritic gneiss

d-c = diorite-charnockite gneiss complex; k = khondalite belt gneiss
see detailed petrographic descriptions in appendix 1.

5.2 Ilmenite compositional variations

Ilmenite was found in 19 of the 22 samples. The three samples where no ilmenite was found, are diorite 2000214, hornblende-biotite gneiss 2000216, and two-pyroxene gabbroic gneiss 2000223; however, in the latter was found one completely altered ilmenite grain. Ilmenite chemistry of the remaining 19 ilmenite-bearing samples are summarized in Figs. 2-6. In terms of TiO_2, a set of samples define a group with low contents (<48 wt. % TiO_2), namely samples charnockite 2000208, hornblende diorites 2000217 and 2000222, and granodiorite 2000224. One other hornblende diorite 2000221 has only yielded one ilmenite grain, with relatively high TiO_2 of about 53 wt.%, and this sample will be disregarded in the following discussion. The group of hornblende diorites, granodiorite and charnockite (200208, 217, 221, 222, 224) appears to form a coherent group with, in addition to low TiO_2, elevated MnO (apart from 2000208), and intermediate to high MgO. MnO is particularly high in the hornblende-bearing sample 2000217 and 2000222 and in the granodioritic gneiss 2000224, with values between 1.5 and 8.7 wt. % MnO. The highest MnO contents are found in ilmenite grains which appear to represent high temperature exsolutions from titanomagnetite. For the ilmenite from the three samples 2000217, 222, and 224, MgO is mostly between 0.5 and 1.7 wt.%. It is noteworthy that all these lithologies are devoid of garnet.

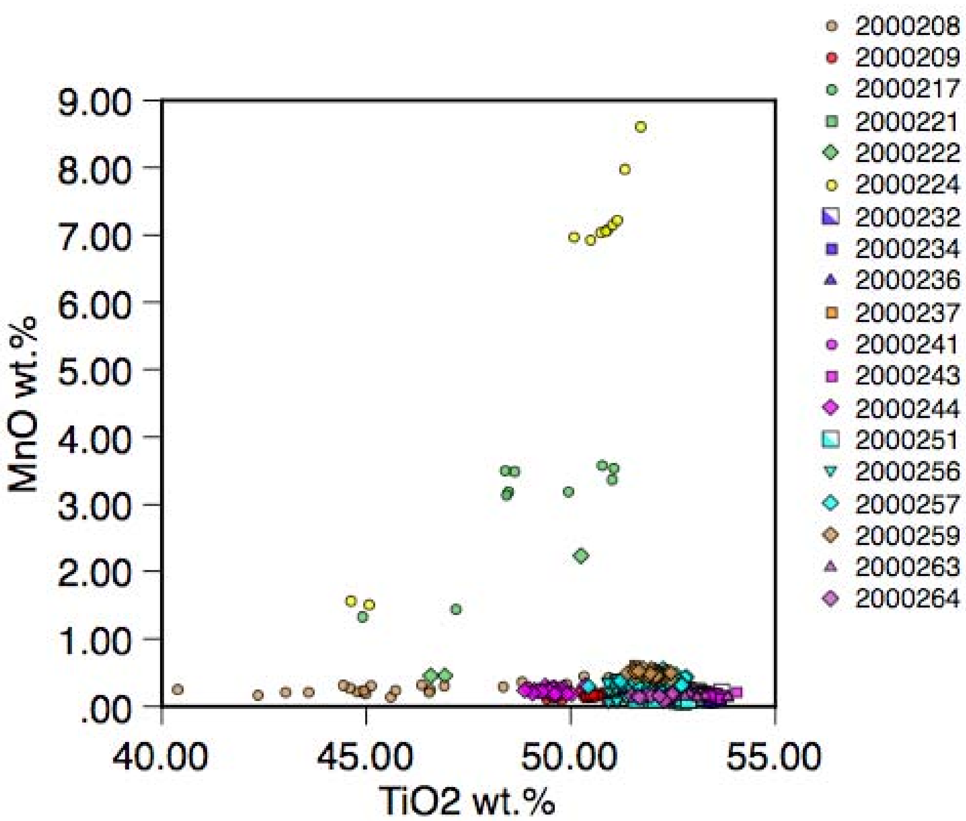

Figure 2. *Variation in chemistry in ilmenite from rock samples.*

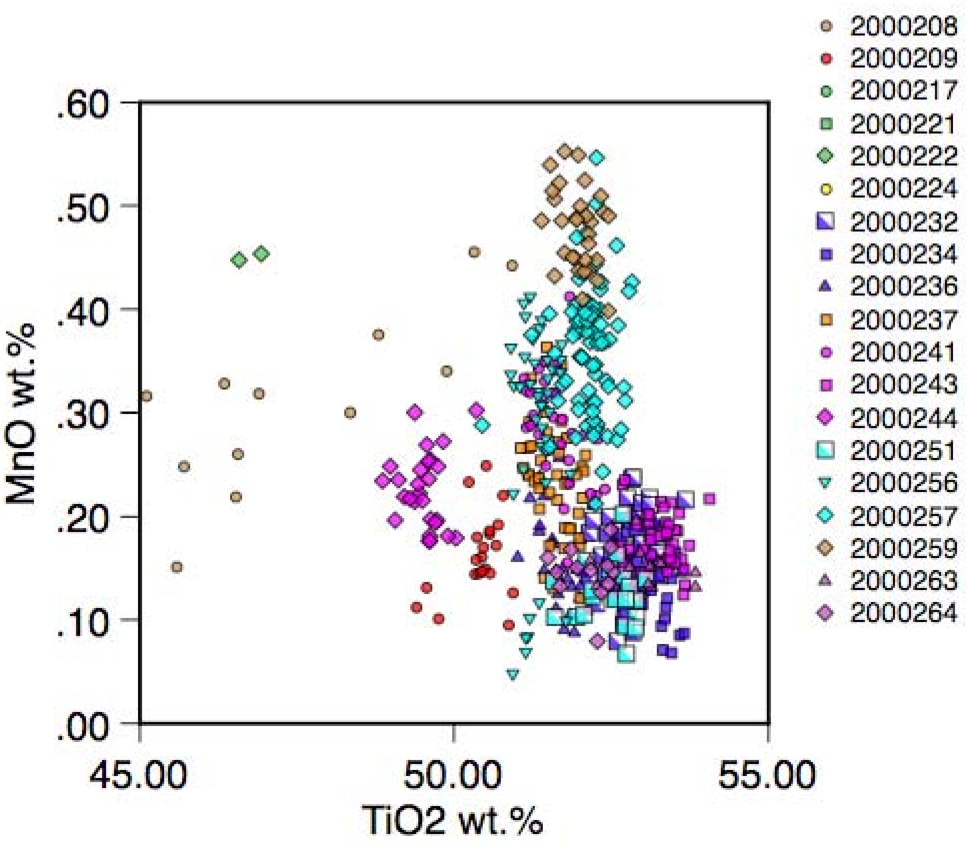

Figure 3. *Variation in chemistry in ilmenite from rock samples. Note the narrow ranges at axes.*

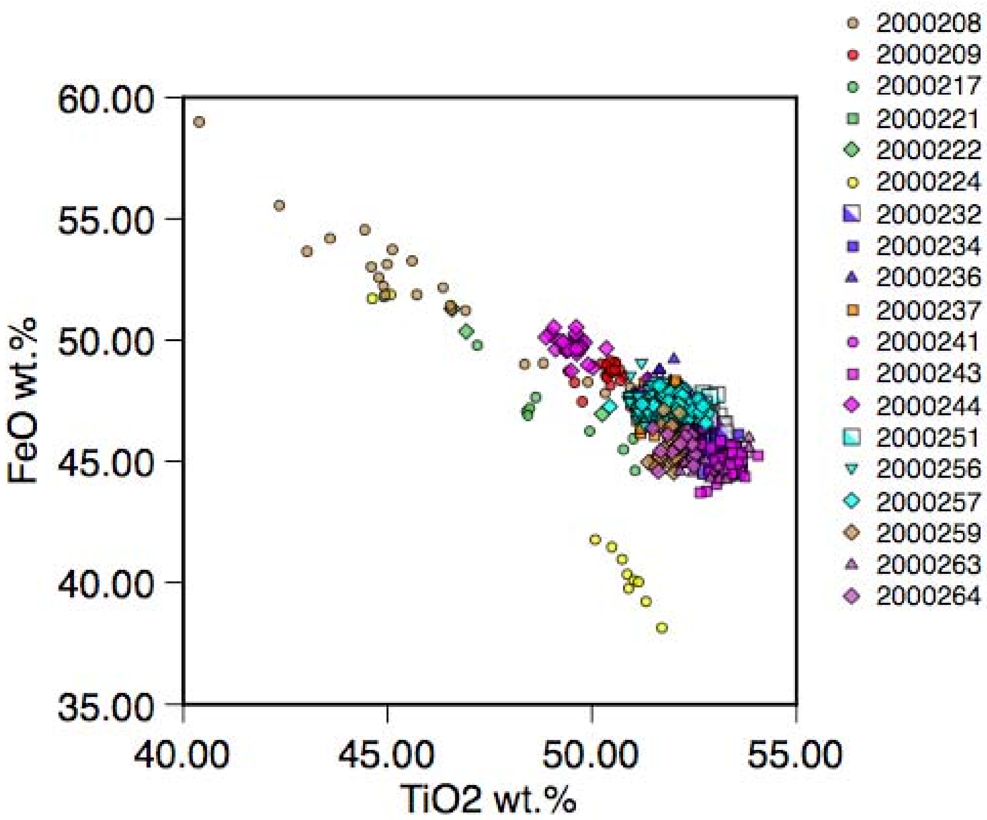

Figure 4. *Variation in chemistry in ilmenite from rock samples.*

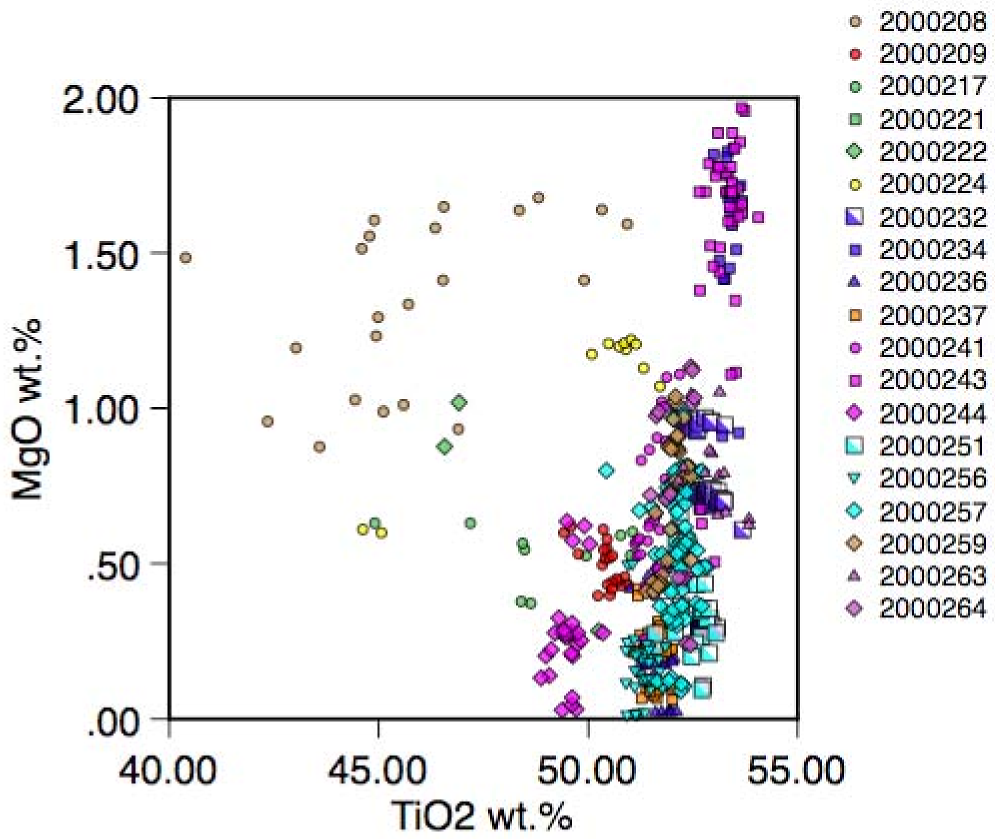

Figure 5. *Variation in chemistry in ilmenite from rock samples.*

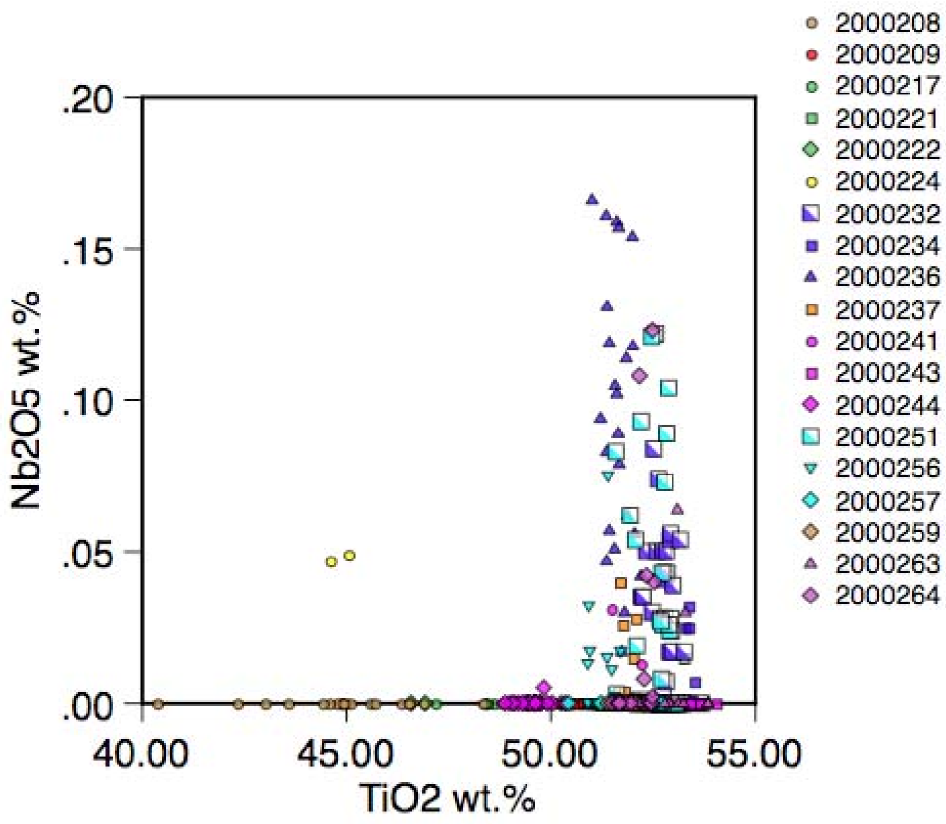

Figure 6. *Variation in chemistry in ilmenite from rock samples.*

In contrast, the remaining samples carrying ilmenites with TiO_2 > 48 wt. % contain garnet (apart from two-pyroxene charnockite gneiss 2000259). Ilmenite in these samples show low MnO (< 0.55 wt.%), but there are some consistent differences within this group (Fig. 3). The orthopyroxene-bearing rocks (2000241, 256, 257, and 259) together define a group with relatively high MnO contents, largely being higher than 0.3 wt.%. Ilmenite from the garnet-bearing lithologies also appear to form a coherent group in terms of FeO contents, whereas ilmenite from the garnet-free rocks mainly fall along a curve with low FeO for a given TiO2 content (Fig. 4). It appears that the low FeO in ilmenite for some of these rocks stems from their content of high MnO. There exists a broad negative correlation between FeO and TiO_2 for ilmenite along the coherent group from garnet-bearing rocks.

In terms of MgO, ilmenite from garnet-bearing rocks show a crude positive correlation, with MgO varying from 0 to 2 wt.% (Fig. 5). A closer inspection of the MgO vs. TiO_2 graph shows that there exists a significant variation in ilmenite composition within individual samples, typically in the order of 0.5 wt. % MgO.

For niobium, the concentration in unaltered ilmenite is commonly at detection level (about 0.01 wt. % Nb_2O_5; Fig. 6). A series of samples show significant, albeit low, concentration of

Nb in the unaltered ilmenite. The samples are particularly 2000236, 251, 264, and 232, with Nb_2O_5 between 0.01 and 0.17 wt. %. Acquisition of Nb during the alteration processes is common, as will be shown below, so it is possible that the ilmenite with elevated Nb_2O_5 are undergoing slight alteration. However, it is interesting to note here, that the first three samples mentioned above out of four samples with Nb_2O_5 > 0.05 wt.% all belong to a group of samples in which no inciepient alteration of ilmenite has been found. Concentrations of the elements Al, Ca, Cr, Si and P are all very low, and show no correlation with TiO_2 (not shown).

5.3 Garnet compositional variations

Out of the 22 samples, 13 samples were found to contain garnet. Of these 13 samples, only one (garnet-clinopyroxene gneiss 2000209) comes from outside the Kerala khondalite belt. The garnet compositions are shown in Fig. 7. Garnet from 2000209 is clearly different in having considerably higher grossular component (about 20%) compared to garnets from the khondalite belt, which all have lower grossular components, namely between 2 and 14%. Three samples from the khondalite belt (2000236, 237, and 256) have garnet with distinctly higher grossular and lower pyrope components (9-14% and 6-13%, respectively) than garnets from the remaining khondalite samples.

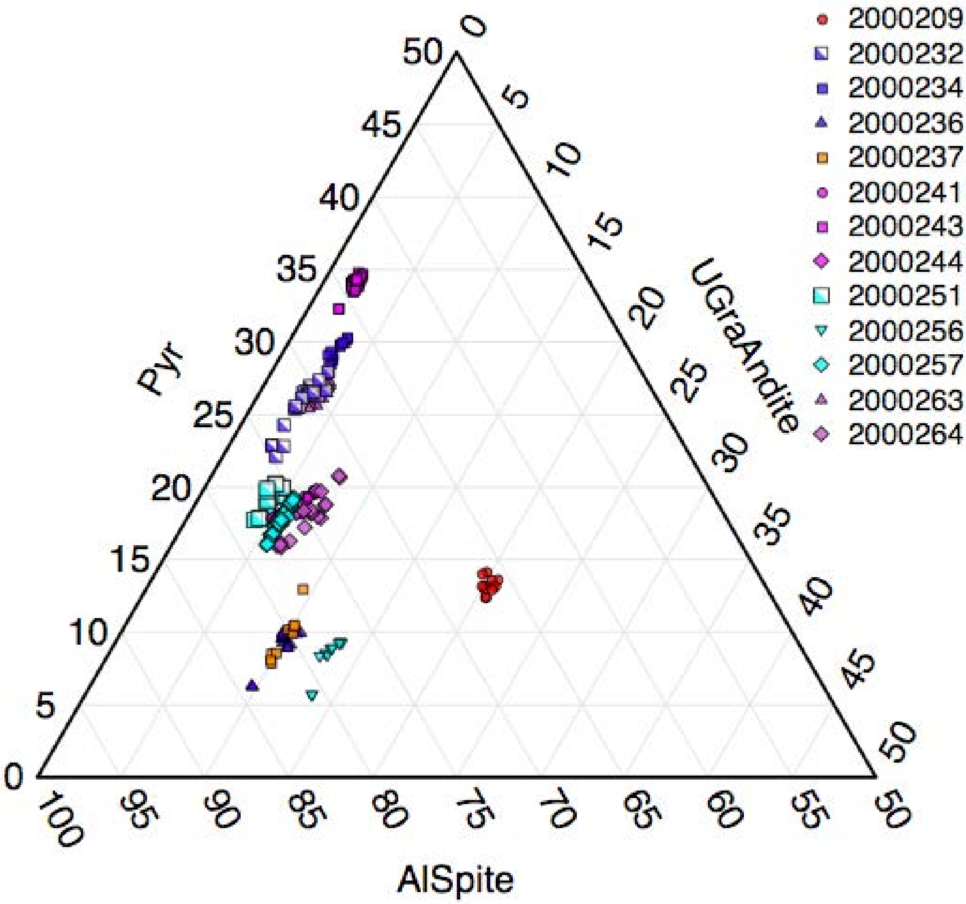

Figure 7. *Variation in garnet chemitry from rock samples, expressed in three components: Ca-garnets UGrAndite, Fe and Mn garnets AlSpite, and Mg garnets Pyr.*

6. Discussion

6.1 Mineral chemistry correlation between sediment and rock samples

In order to provide an overview of the chemical characteristics of the minerals ilmenite and garnet from the sediment and the rock samples, average mineral compositions have been calculated. It is important here to bear in mind that the mineral data for rock samples and for sediment samples differ in several respects. Compared to the rock samples, the sediment samples by nature contain suites of minerals from many lithologies, which have undergone series of low temperature processes, including alteration, during erosion, transport and sedimentation. The sediment minerals were identified automatically by the CCSEM on the basis of their chemistry and subjected to an EDS analysis with short counting time, yielding poor counting statistics. Thus, the analytical error on the CCSEM analyses is considerably larger than the electron micro-probe data obtained on minerals from rock samples. Also, the minerals subjected to micro-probe analysis from the rock samples, were all individually identified using backscatter imaging. Therefore, in the following, only elements with concentrations above the detection limit of the CCSEM routine (approximately 0.2 wt. %) are considered. An example of this is given in Fig. 8, showing that the average P_2O_5 of between 0.08 and 0.2 wt. % for ilmenite analysed by the CCSEM probably are unreastically high, because all ilmenite analyses from the rock samples lie close to the detection limit of the electron micro-probe of about 0.01 wt. % P_2O_5.

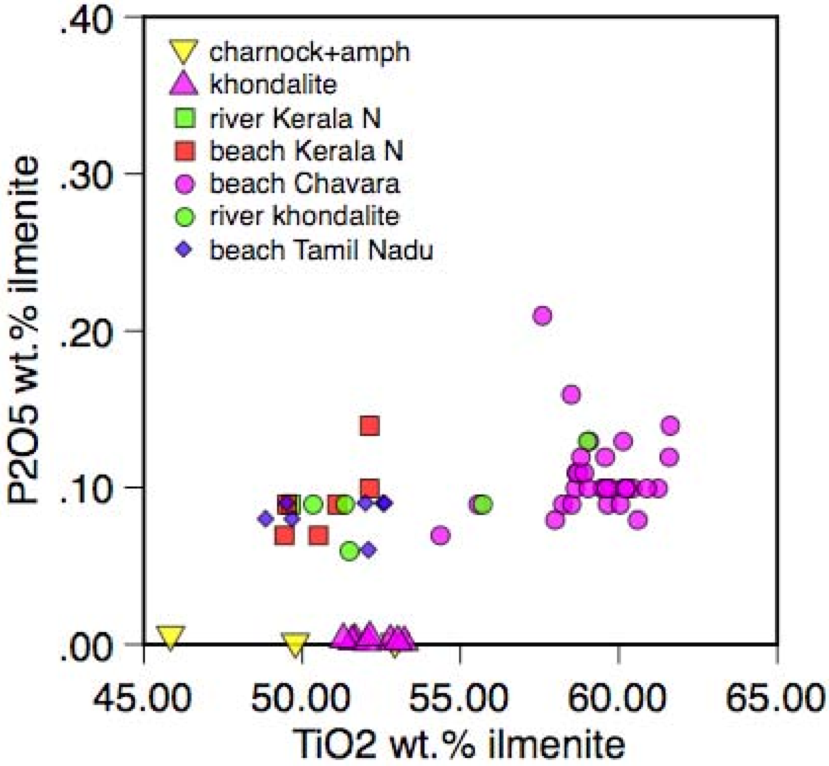

Figure 8. *Comparison of average ilmenite compositions as measured with the electron micro-probe on ilmenite from rock samples (triangles) and with the CCSEM on ilmenite from sediments (circles, squares and diamonds).*

6.2 Magnesium in ilmenite

One of the key elements suggested by Bernstein (2003) to describe compositional variation in ilmenite from beach and river sediments is magnesium. It was shown that high MgO (>0.8 wt.%) in ilmenite suggested an origin within the khondalite lithologies. The MgO content for ilmenite from sediment and rock samples are summarized in Fig. 9. From the data presented above, it is clear that ilmenite from the rock samples show large variations in MgO, and the khondalite samples appear to span the entire range in MgO. There is one group of rock samples from the khondalite belt (2000232, 241, 257, 259, 263, 264) with ilmenite containing intermediate amounts of MgO (0.6-0.8 wt. %). Other samples either have higher (2000234, 243 at about 1.5 wt. % MgO) or much lower (<0.3 wt. % MgO). For the elements, Al and Mn, it appears that the recorded values in average ilmenite from sediments are much higher than those from rock samples, which in turn have concentrations at or lower than the detection limit for the CCSEM (Fig. 10 and 11). An exception to this scheme, is the high MnO recorded in average ilmenite from some gneiss samples from the Northen Kerala which have MnO bwetween 1 and 6.3 wt. %. This elevated MnO content accords at least qualitatively witht he higher MnO in beach and river samples from the northern Kerala State (Fig. 11), which have MnO between 1 and 2 wt.% in average ilmenite. All beach sediments containing ilmenite with elevated TiO_2 (Chavara deposits) and sediments from rivers within the khondalite belt contain ilmenite with uniform and low MnO of about 0.5 wt. %.

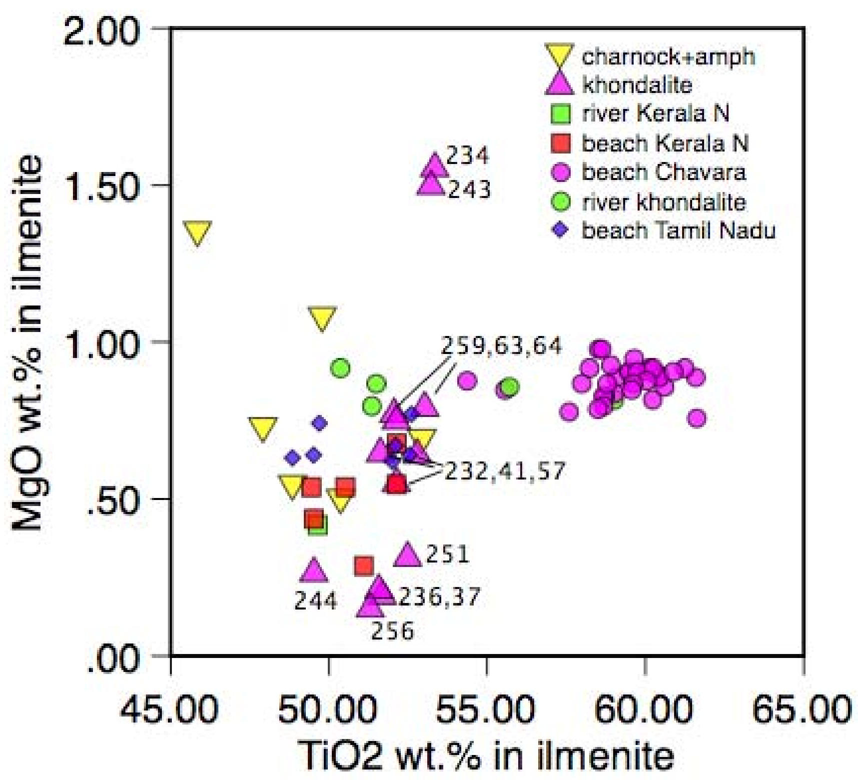

Figure 9. *Comparison of average ilmenite compositions as measured with the electron micro-probe on ilmenite from rock samples (triangles) and with the CCSEM on ilmenite from sediments (circles, squares and diamonds).*

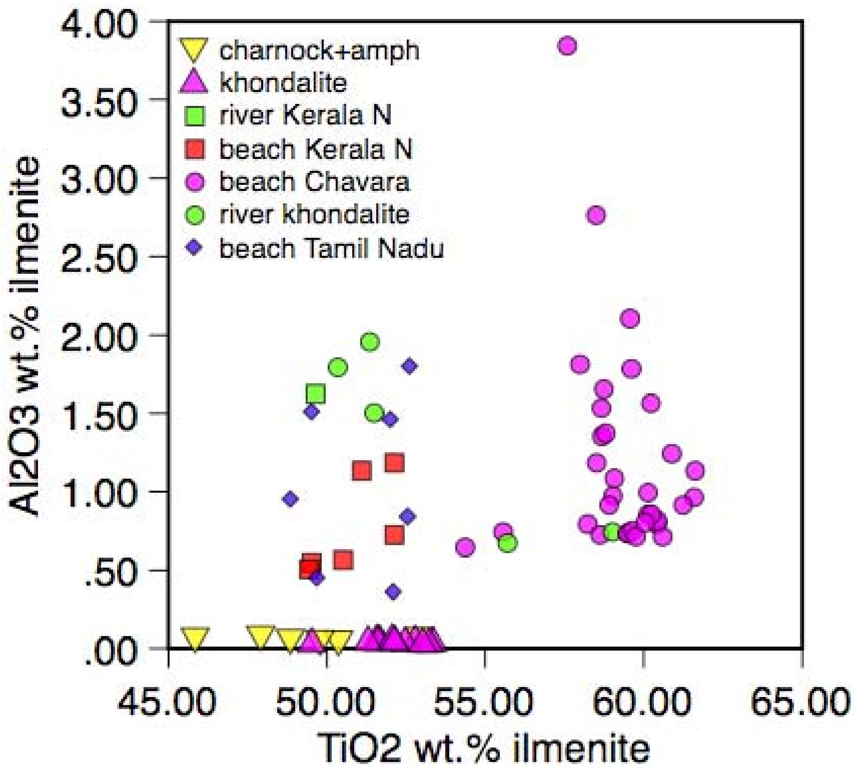

Figure 10. *Comparison of average ilmenite compositions as measured with the electron micro-probe on ilmenite from rock samples (triangles) and with the CCSEM on ilmenite from sediments (circles, squares and diamonds).*

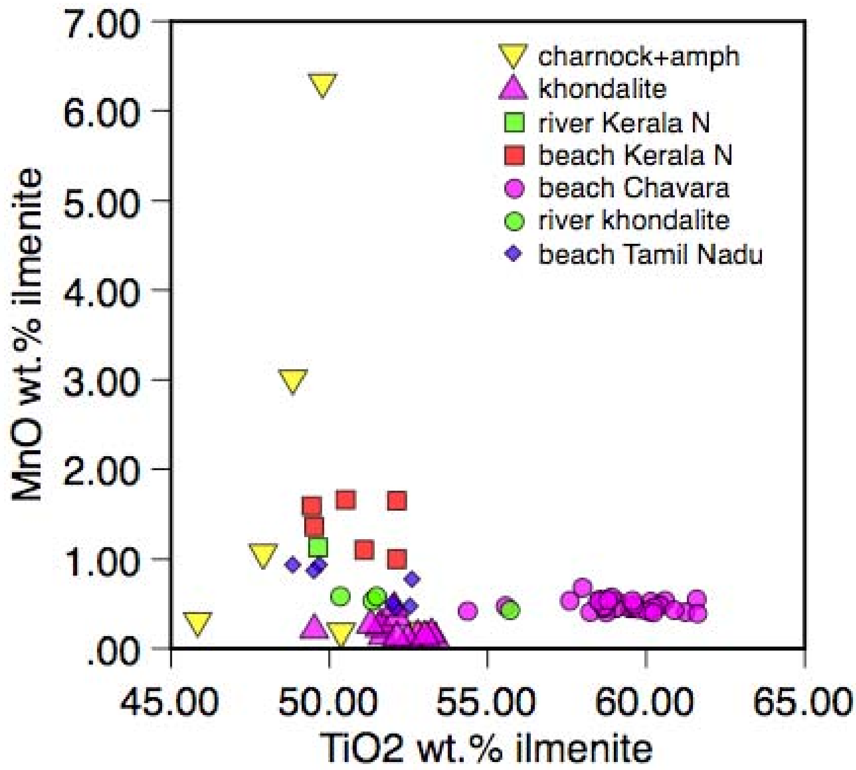

Figure 11. *Comparison of average ilmenite compositions as measured with the electron micro-probe on ilmenite from rock samples (triangles) and with the CCSEM on ilmenite from sediments (circles, squares and diamonds).*

Thus, based on the combined CCSEM data on sediments and electron micro-probe data on rock samples, ilmenite chemistry alone apparently does not establish a clear link between sediment ilmenite and possible source rock. On a broad scale, however, one can say that the low MnO both in ilmenite with elevated TiO_2 from the southern Kerala State coasts and in ilmenite from all analysed rocks from the khondalite belt and the general higher TiO_2 for unaltered ilmenite from khondalite lithologies to some extend confirms the view that these are the sources for the high grade ilmenite in beach sediments. In terms of MgO, one hypothesis could be that the high grade ilmenite in beach sediments are mainly derived from the khondalite rock samples with intermediate MgO between 0.6 and 0.8 wt.% MgO. This hypothesis can be tested by considering the garnet chemistry.

6.3 Garnet chemistry

In Fig. 12 average garnet composition are displayed. It is evident that sediment samples from beaches and rivers from north Kerala State (squares in figure) have average garnet compositions with intermediate to high grossular components (7-17%) and plot towards the garnet composition of the single rock sample representative for the lithologies outside the khondalite belt, 2000209. Similar high grossular components are known from garnets of two-pyroxene charnockites and mafic granulites (data from Chacko et al., 1987; Nandakumar & Harley, 2000 and Sabeen et al., 2002), as presented by the green field in Fig. 12. Sediments from Tamil Nadu coast contain garnets with relatively constant grossular components of 3-5%, but varied pyrope components of 18-28%. Garnet averages from sediments containing high Ti ilmenite from the SW Kerala State coastline (including the Chavara deposit) show a very limited compositional range with 2-4% grossular and 24-30% pyrope ('beach Chavara' in legend). Published garnet compositions of khondalite belt lithologies are presented in Fig. 12 by the blue field, encompassing sillimanite-bearing schists and orthopyroxene-bearing gneisses (data from Chacko et al., 1987; Nandakumar & Harley, 2000 and Sabeen et al., 2002). Compared to average garnets from our rock samples of the khondalite belt, the detrital garnet data corresponds to the high pyrope lithologies, represented by the samples 2000232, 234, and 263. One interpretation of this correspondance in average garnet compositions could be that the source for the high Ti ilmenite is found in these type of gneisses. However, this interpretation is only partly supported by the considerations on ilmenite chemistry stated above, since, of the three rock samples 2000232, 234, and 263, two samples (200232 and 263) have ilmenite with intermediate MgO of 0.6-0.8 wt.%, while sample 200234 has ilmenite with very high MgO of 1.6 wt.% (Fig. 9). On the other hand, the ilmenite-garnet compositional relationships does place some constraints on the possible sources of high Ti ilmenite. Considering the MgO-TiO_2 relationship in Fig. 9, it is seen that the among the group of rock samples with low-MgO ilmenite are found the three samples 200236, 237, and 256, which are also characterized by having very low pyrope contents (Fig. 12). The sediment samples with high Ti ilmenite appear to contain very few garnets, if any, of this composition, and therefore are these lithologies *unlikely* to be major sources of ilmenite.

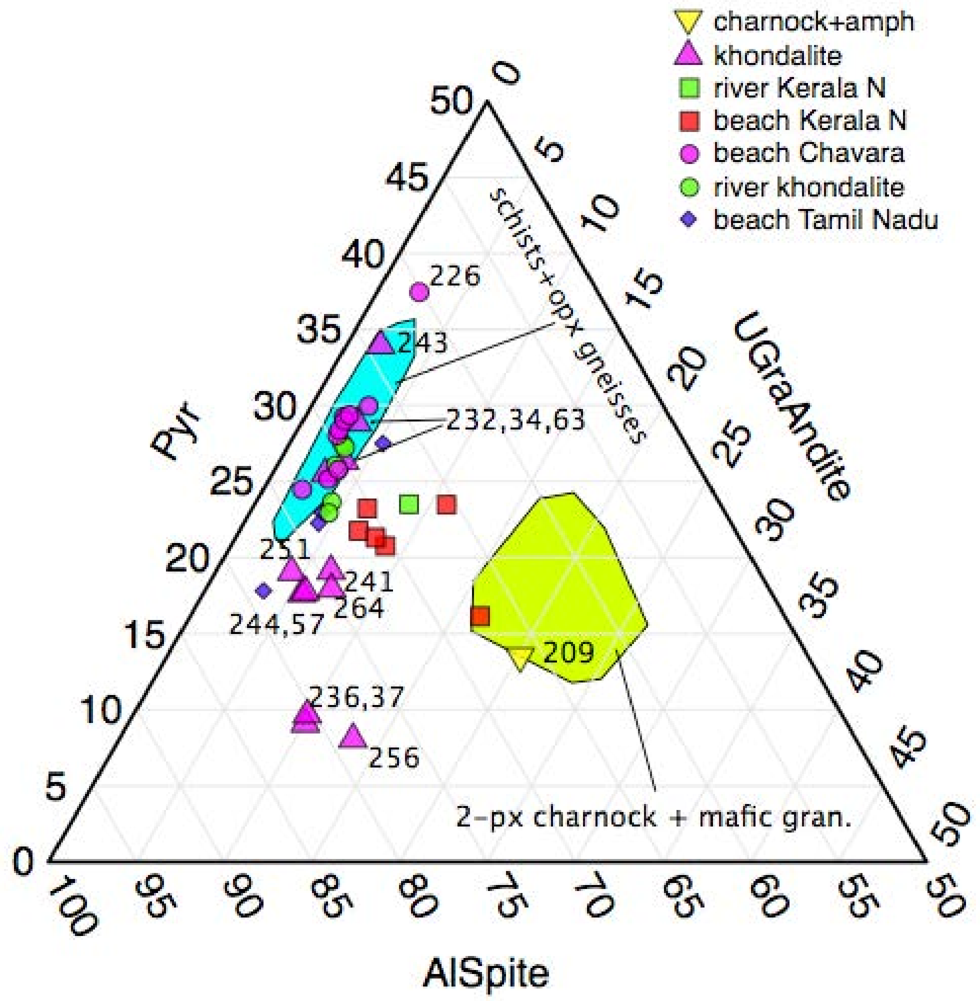

Figure 12. *Average garnet compositions from rock samples (triangles) and sediments (circles, squares and diamonds). Shown are also fields of published garnet compositions from rocks of Kerala State (Chacko et al., 1987, Nandakumar and Harley, 2000; Sabeen et al., 2002).*

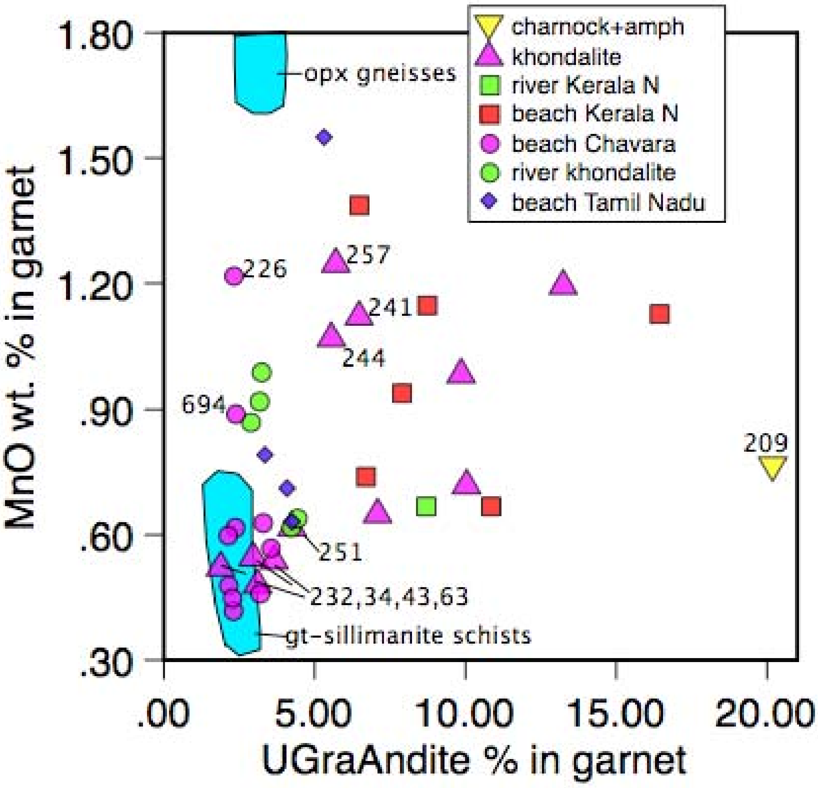

Figure 13. *Average garnet compositions from rock samples (triangles) and sediments (circles, squares and diamonds). Shown are also fields of published garnet compositions from rocks of Kerala State (references given in Fig. 12).*

Additional information on possible sources for the high Ti ilmenite sediment can be extracted from manganese contents of garnets. As illustrated in Fig. 13, most of the garnets from sediment samples with high Ti ilmenite are characterized by having low contents of MnO along with their low grossular components as stated above. Garnet from one sediment samples has elevated MnO of about 1.2 wt.%, and this sample (2000226) also shows the highest recorded pyrope component in the average garnet (Fig. 12). However, there are only 6 recorded garnet CCSEM analyses for this sample, and the MnO varies from 0.2 to 2.0 wt.%, and hence this sample is disregarded in the following discussion. One sediment sample (2000694) has garnet with intermediate MnO of 0.9 wt.%, and thus similar to garnets from three river samples, but all remaining sediment samples with high Ti ilmenite , including the one river sediment sample 2000253 contain garnets with uniformly low MnO of 0.4-0.6 wt. %. Garnets from five rock samples have similarly low manganese contents, namely 2000232, 34, 43. 51, and 63 - and all these samples, except 2000251, share the features of having garnets with high pyrope (Fig. 12) and having ilmenite with high or intermediate MgO (Fig. 9). The group of rock samples (2000241, 244, 257) having garnet with intermediate compositions of between 17 and 19 % pyrope (Fig. 12) and having ilmenite with low to intermediate MgO of 0.3 to 0.6 wt. % clearly have too high MnO in their garnets (1.1-1.3 wt. %) to be possible sources for sediments with high Ti ilmenite.

On the basis of garnet and ilmenite compositional characteristics, it is therefore concluded that lithologies like those represented by samples 2000232, 34, 43, and 63, are the main sources for high Ti ilmenite along the south Kerala state coastline.
The four samples are characterized by having relatively large amounts of garnet, and by containing biotite and appreciable amounts (ca. 5 vol. %) of ilmenite. Also, 2000232 and 34 contain sillimanite, which is not found in any other of the rock samples. Finally, these four samples show absence of orthopyroxene, which is found in most other lithologies in the khondalite belt.

The low MnO garnets appear to be a common feature for garnet-sillimanite schists, since all low MnO garnets reported by Nandakumar and Harley (2000) comes from this group of rocks (Fig. 13), distinct from the high MnO (1.6-3.5 wt.% recorded by garnets from orthopyroxene-bearing gneisses from within the khondalite belt.
It is difficult to estimate how representative the four samples with low MnO garnets from our collection are in terms of the khondalite lithologies. Sediments from the river systems appear to collect garnets from several sources, since their garnet compositions are intermediate between garnets from these four lileky source rocks and garnets from other lithologies with elevated MnO (Figs. 9 and 13). In some of the sediment samples from the Chavara ilmenite deposits, there are found a few garnets with high MnO contents (2-5 wt.%) and it may be that the bimodal garnet population of sediment sample 2000226 simply reflects derivation of garnets from the two main gneiss sources. The dominance of garnets from sillimanite-bearing schists in the sediments with high Ti ilmenite may reflect that the sillimanite-bearing schists in general are more garnet rich, and that these lithologies, being more foliated and having well developed schistosity are more prone to erosion than the more competent and massive orthopyroxene bearing gneisses.

7. Ilmenite alteration in rock samples

In several samples, ilmenite grains show signs of alteration. The alteration changes the composition of the ilmenite towards elevated Ti contents. In order to explore the nature of this alteration, several grains from 5 samples were selected for detailed analytical traverses across the alteration front, from the unaltered ilmenite into the alteration zone.

7.1 Textures and electron-microprobe traverses

Sample 2000224 - granodioritic gneiss (diorite-granite-charnockite gneiss, N Kerala)
The analysed grain appears to represent a high temperature exsolution from titanomagnetite. The grain is about 50 μm across (short dimension), and the traverse runs from the altered corner and about 20 μm into the unaltered ilmenite grain (Fig. 14). The unaltered grain has 51 wt. % TiO_2 and high MgO and MnO contents (1.2 and 7.5 wt.%, respectively), which are among the highest recorded in this study (Fig. 15). By entering the alteration zone, from the unaltered ilmenite, MnO firstly increases to 13 wt. % and then drops to about 4 wt. %, while MgO drops to about 0.6 wt. % and FeO drops to 28-30 wt. %. There are slight increases in SiO_2 and Al_2O_3, while CaO, P_2O_5, Cr_2O_3 and Nb_2O_5 all are around detection limits.

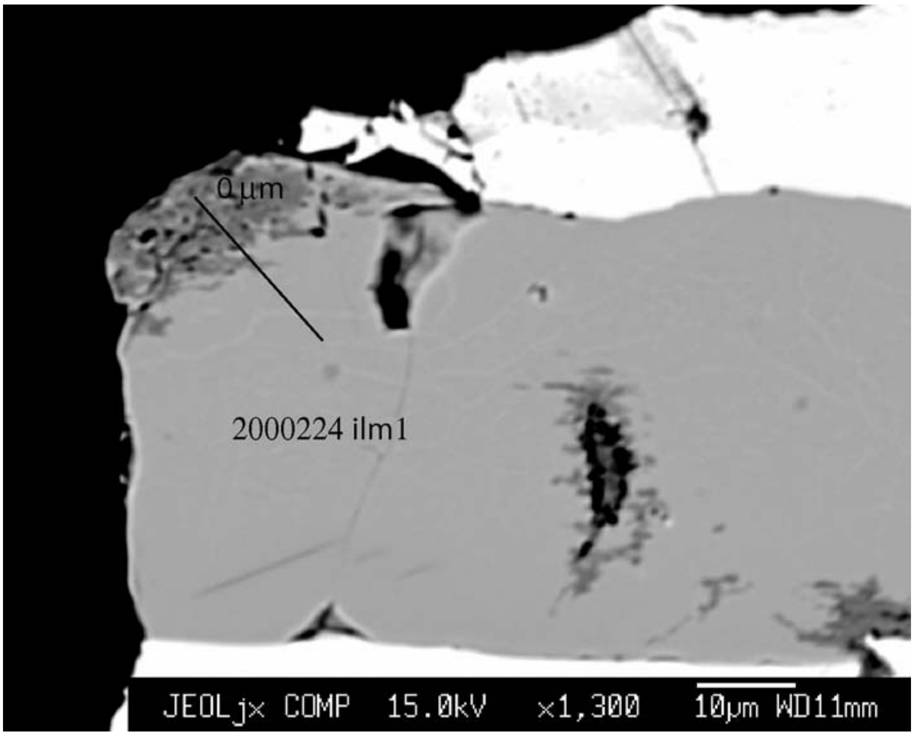

Figure 14. *Altered ilmenite exsolution from titanomagnetite, sample 2000224. The titanomagnetite is seen at the upper and lower part of the photo.*

traverse ilm1, sample 2000224

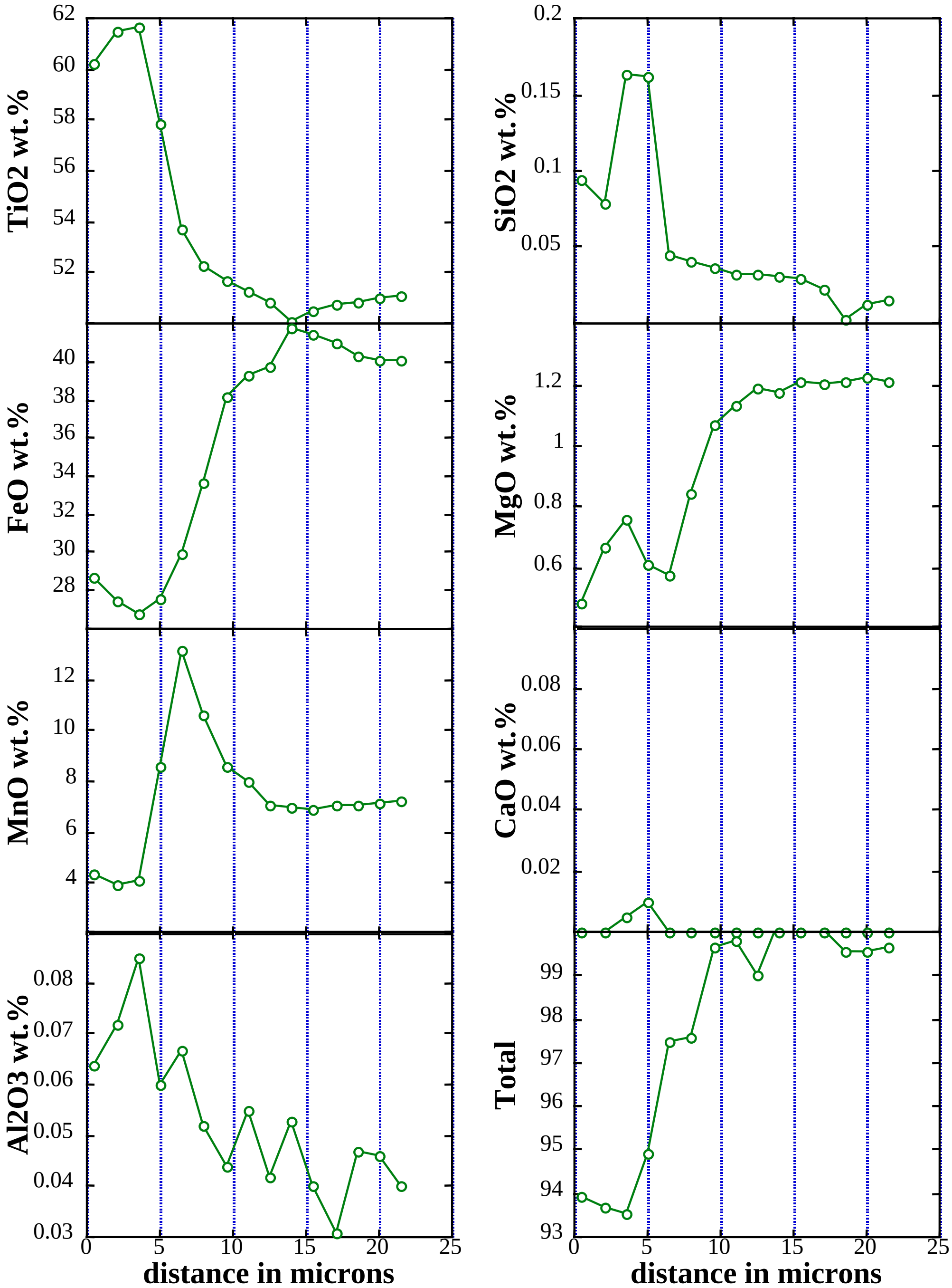

Figure 15a.

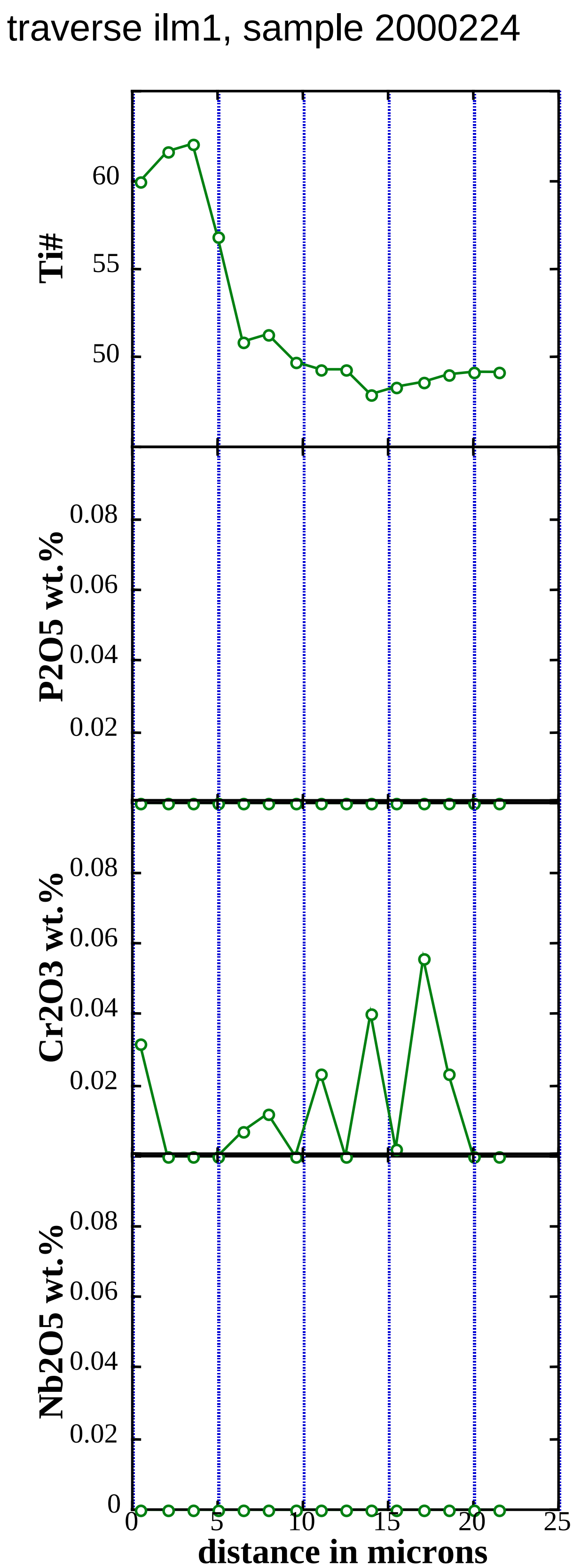
traverse ilm1, sample 2000224
Ti#
60
55
50
P2O5 wt.%
0.08
0.06
0.04
0.02
Cr2O3 wt.%
0.08
0.06
0.04
0.02
Nb2O5 wt.%
0.08
0.06
0.04
0.02
0
0
5
10
15
20
25
distance in microns

Figure 15b.

Sample 2000232 - garnetiferous quatzo-felspathic gneiss (khondalite belt).
In this sample four grains were analysed, three altered ilmenite (ilm1, 2, and 4) and one grain (ilm3) of completely altered ilmenite.

Ilmenite grain ilm1 is a about 150 μm across, and shows alteration along one grain boundary (Fig. 16). The analytical traverse shows that the unaltered ilmenite has about 53 wt. % TiO_2 and low MnO (about 0.15 wt. %) and intermediate MgO of about 0.7 wt. % (Fig. 17). All other analysed elements apart from Fe are below detection limit. When entering the alteration zone, TiO_2 jumps to nearly 90 wt.%, but within the alteration zone, TiO_2 falls to a more moderate level of between 60 and 65 wt. %. The variation in FeO shows a similar pattern, but with negative correlation with TiO_2. The elements Al_2O_3, MnO, P_2O_5, and Cr_2O_3 show little change from the unaltered ilmenite to the altered zone, while SiO_2, MgO, CaO, and Nb_2O_5 all show significant increases, but also with some variation. Analytical total drops to a steady 85 wt.% in the alteration zone.

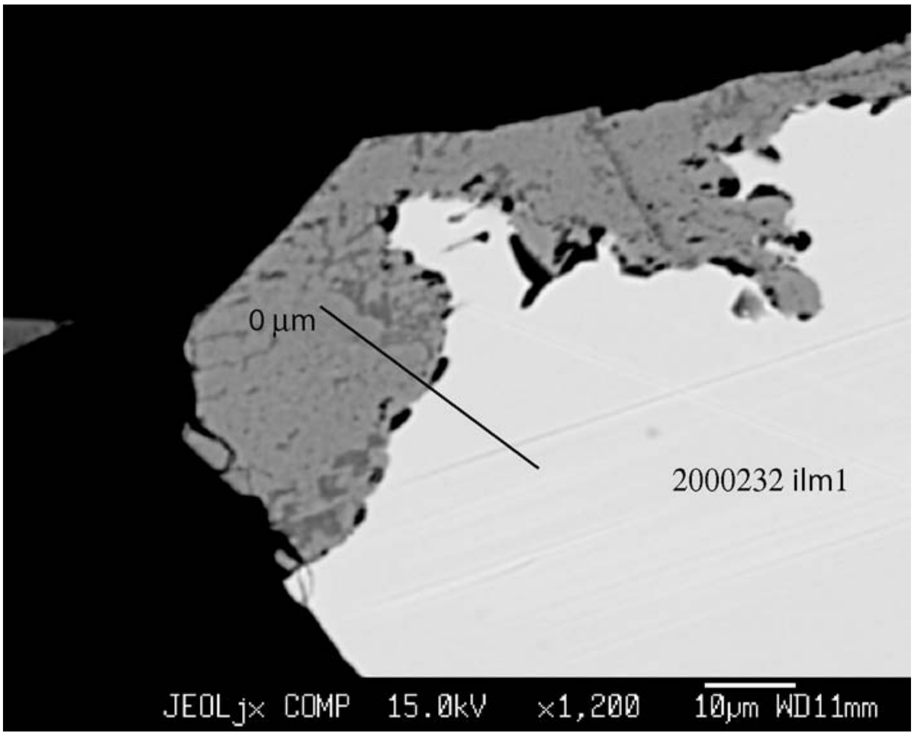

Figure 16. *Alteration along ilmenite grain boundary, sample 2000232.*

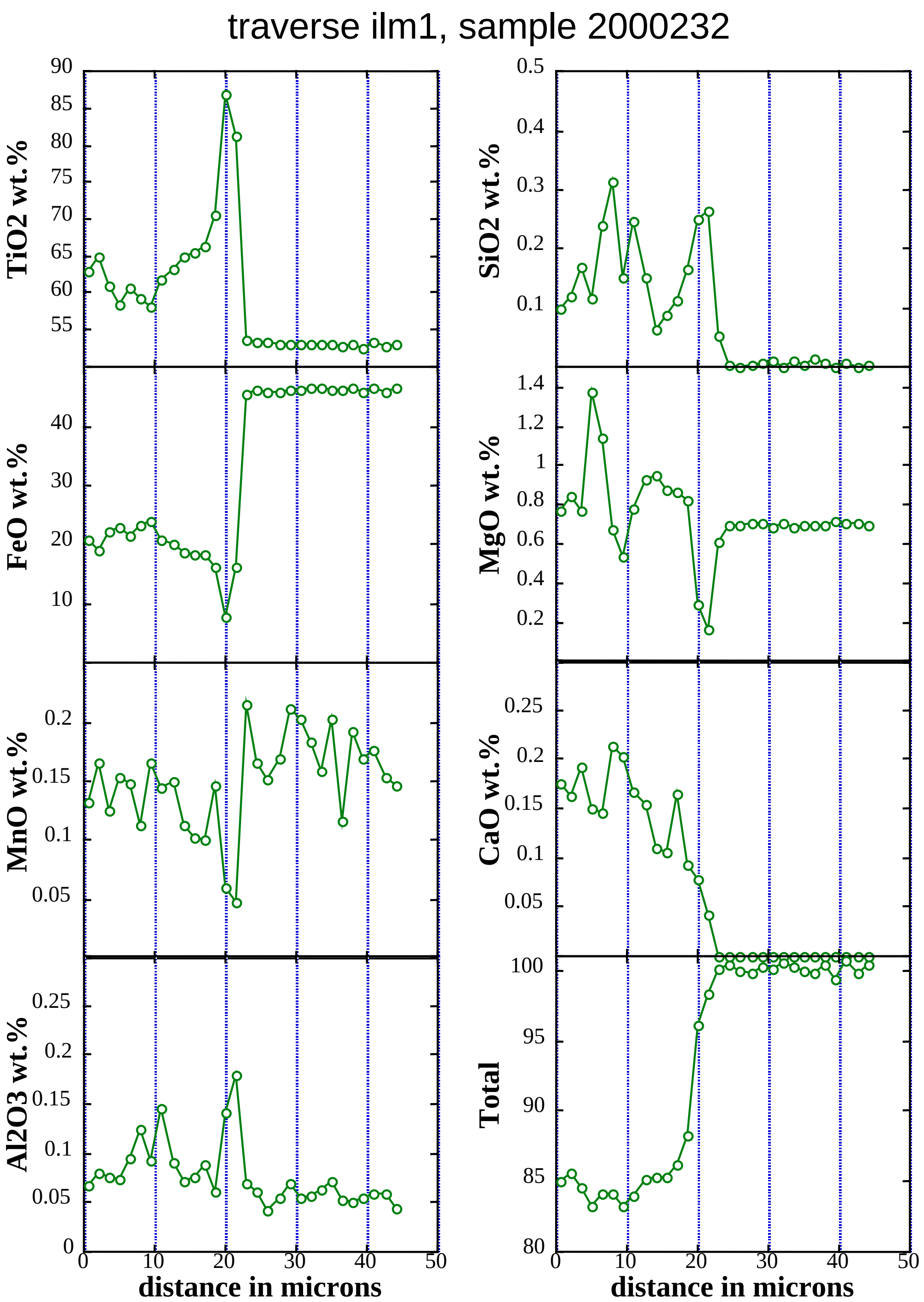
traverse ilm1, sample 2000232
TiO2 wt.%
SiO2 wt.%
FeO wt.%
MgO wt.%
MnO wt.%
CaO wt.%
Al2O3 wt.%
Total
distance in microns
distance in microns

Figure 17a.

traverse ilm1, sample 2000232

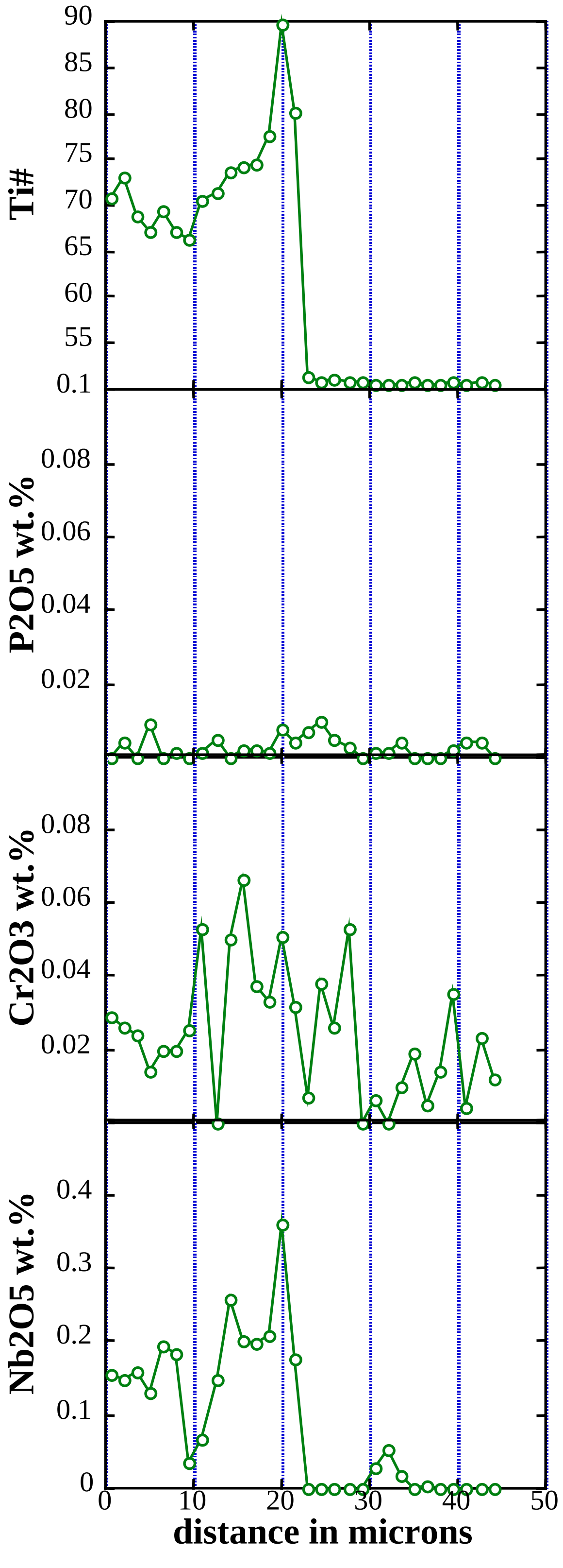

Figure 17b.

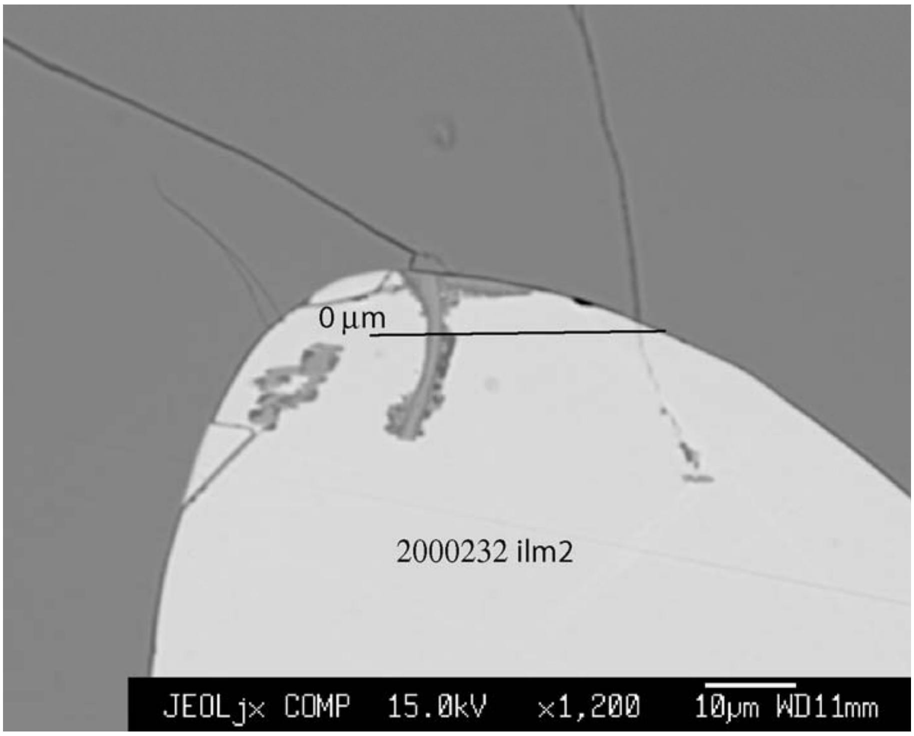

Figure 18. *Alteration of ilmenite along grain boundary to garnet (dark grey) and along fracture. Sample 2000232.*

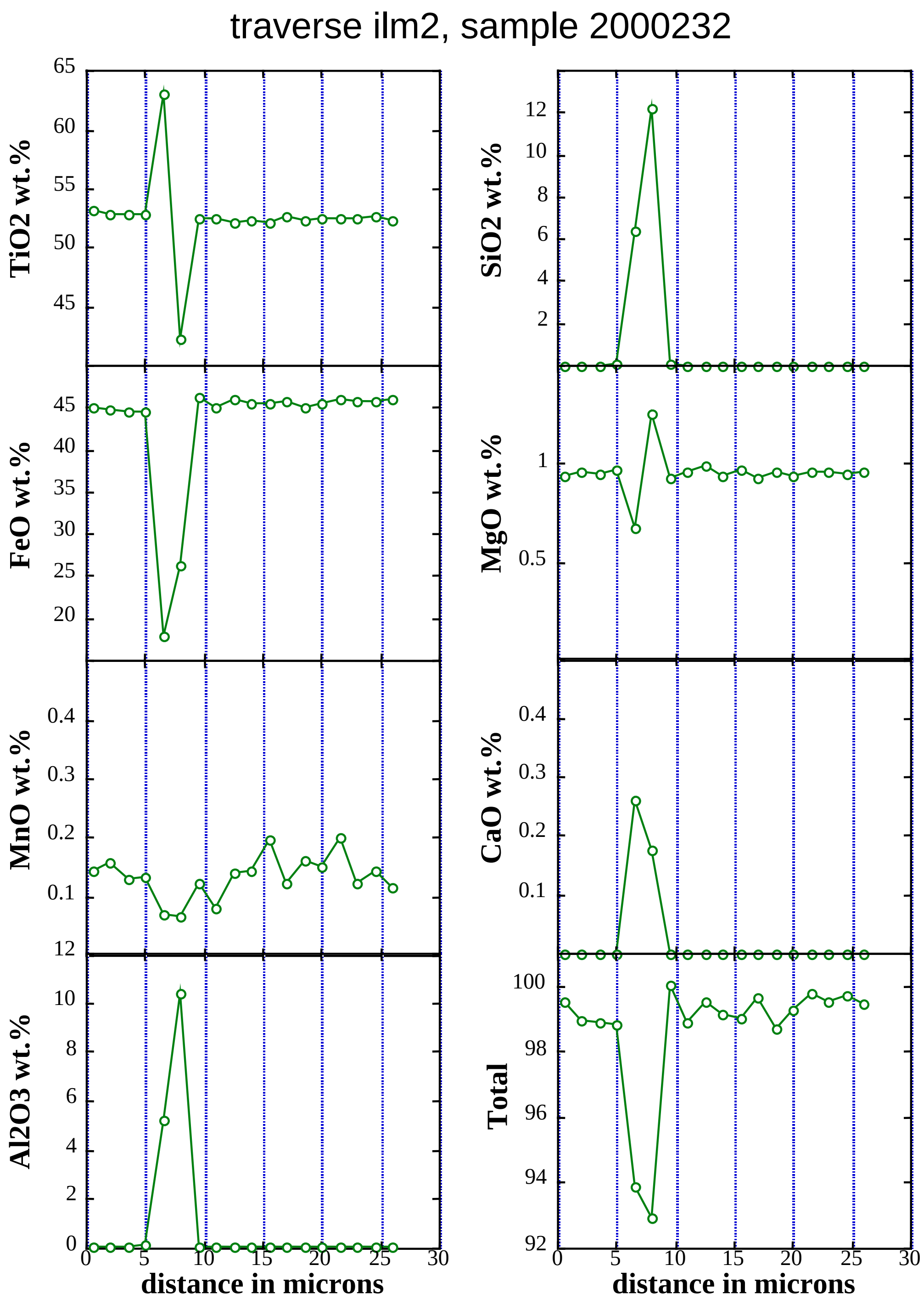
traverse ilm2, sample 2000232
TiO2 wt.%
SiO2 wt.%
FeO wt.%
MgO wt.%
MnO wt.%
CaO wt.%
Al2O3 wt.%
Total
distance in microns
distance in microns

Figure 19a.

traverse ilm2, sample 2000232

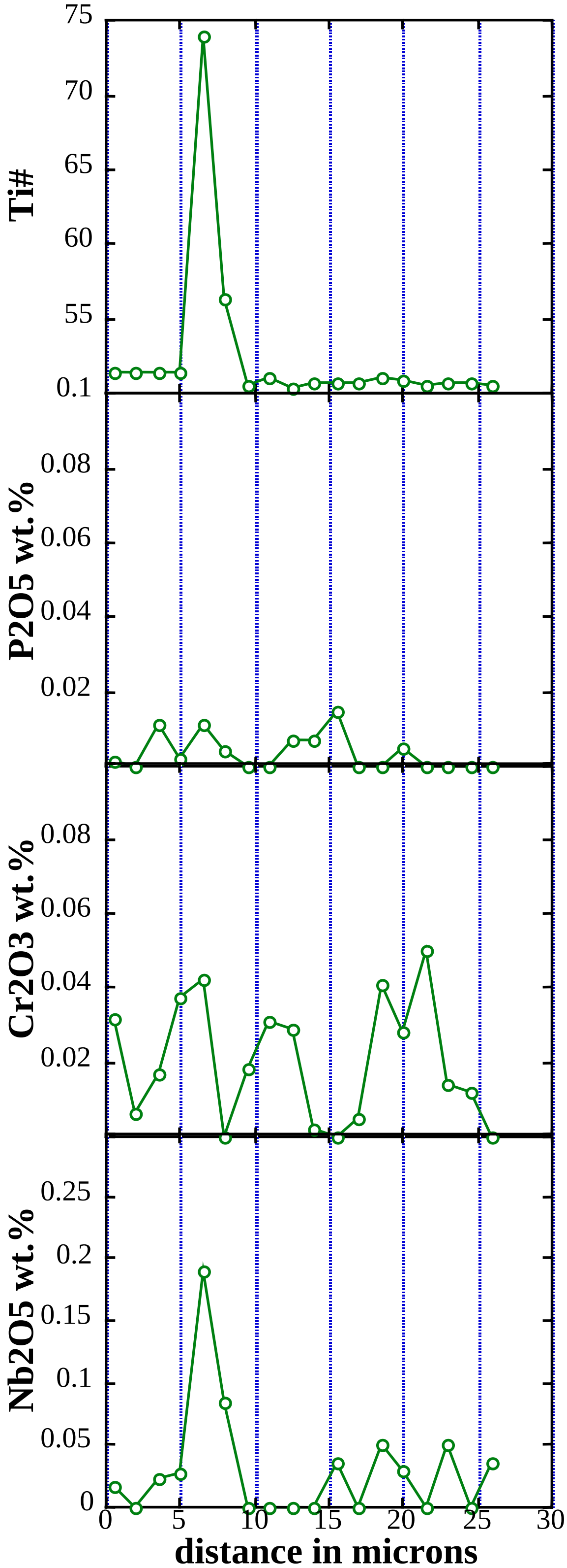

Figure 19b.

Ilmenite grain ilm2 borders to a garnet grain, and as can be seen on Fig. 18, the ilmenite grain shows incipient alteration along one fracture that proceeds from the garnet into the ilmenite grain. The traverse across this feature shows that one part of the alteration halo around the fracture is dominated by a TiO_2 and FeO poor, and Al_2O_3, SiO_2, MgO, CaO rich zone (Fig. 19). The other part of the fracture has a TiO_2, Al_2O_3, SiO_2, CaO, and Nb_2O_5 rich zone. The unaltered ilmenite grain has about 53 wt. TiO_2, low MnO of about 0.15 wt.%, and very low concentrations of the other elements, apart from FeO and from MgO, of which MgO is high at around 1 wt.%.

The ilm3 grain represents mainly pseudorutile, with a spongy appearence (Fig. 20). The grain, which is some 200 μm across, shows a series of lamellae oriented in a parallel fashion, that suggests they represent stages of alteration from an original ilmenite grain. The traverse runs across these lamellae, and shows that the lamellae are characterized by highly variable concentrations of TiO_2 (45-90 wt. %), variably and high Al_2O_3, SiO_2, FeO, and MgO, while CaO, MnO, P_2O_5, Cr_2O_3, and Nb_2O_5 are low (Fig. 21). The areas with less well developed lamellae are characterized by less variable concentrations of TiO_2 (high), and FeO, Al_2O_3, SiO_2, and MgO (low).

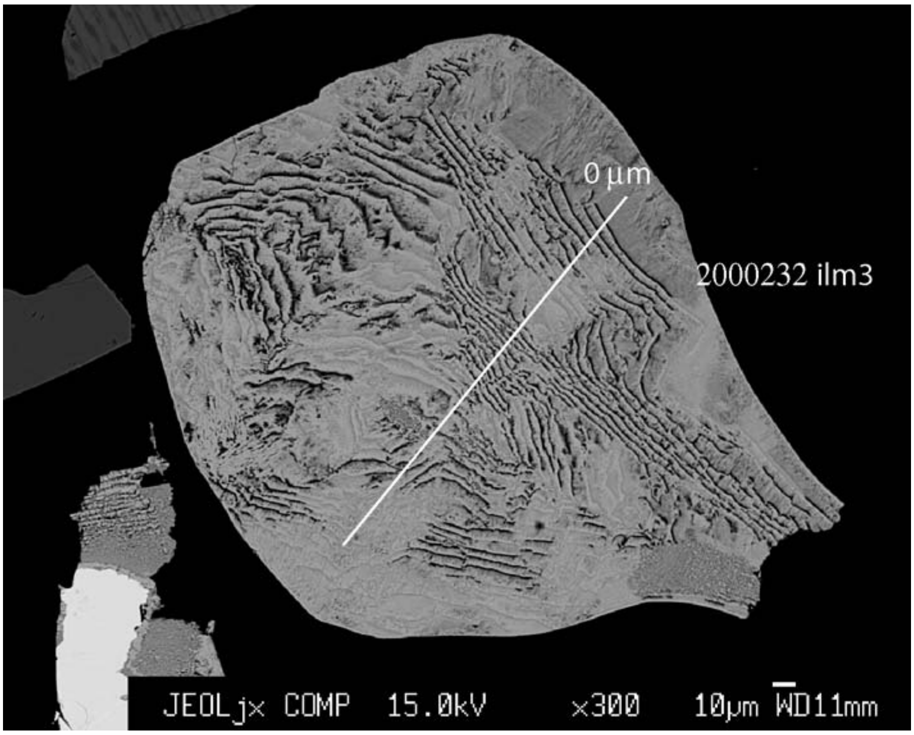

Figure 20. *Complete alteration of ilmenite to pseudo-rutile following epitaxial planes. Note grain 2000232 ilm4 in the lower left of the photo. Sample 2000232.*

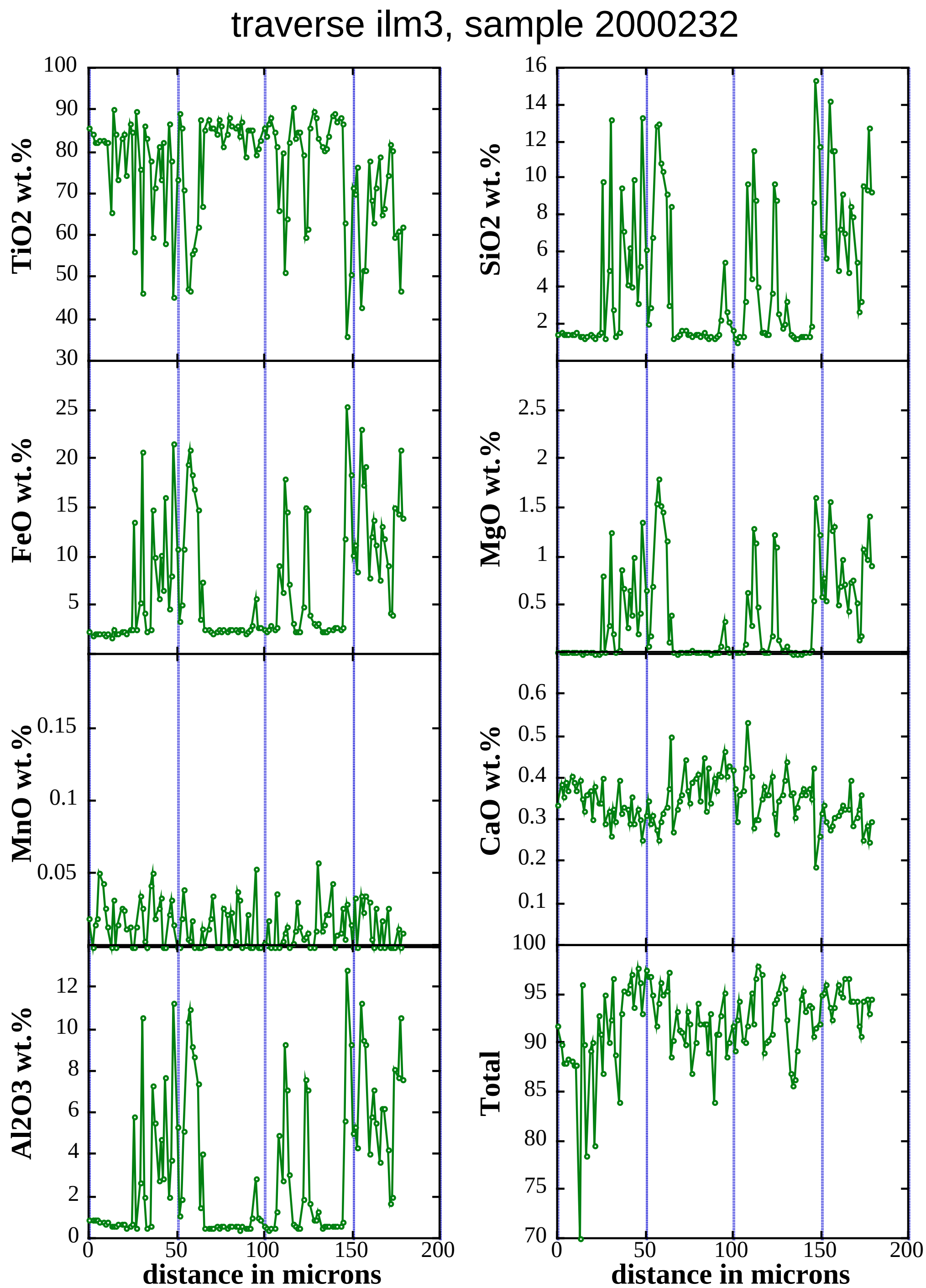
traverse ilm3, sample 2000232
TiO2 wt. %
SiO2 wt. %
FeO wt. %
MgO wt. %
MnO wt. %
CaO wt. %
Al2O3 wt. %
Total
distance in microns
distance in microns

Figure 21a.

traverse ilm3, sample 2000232

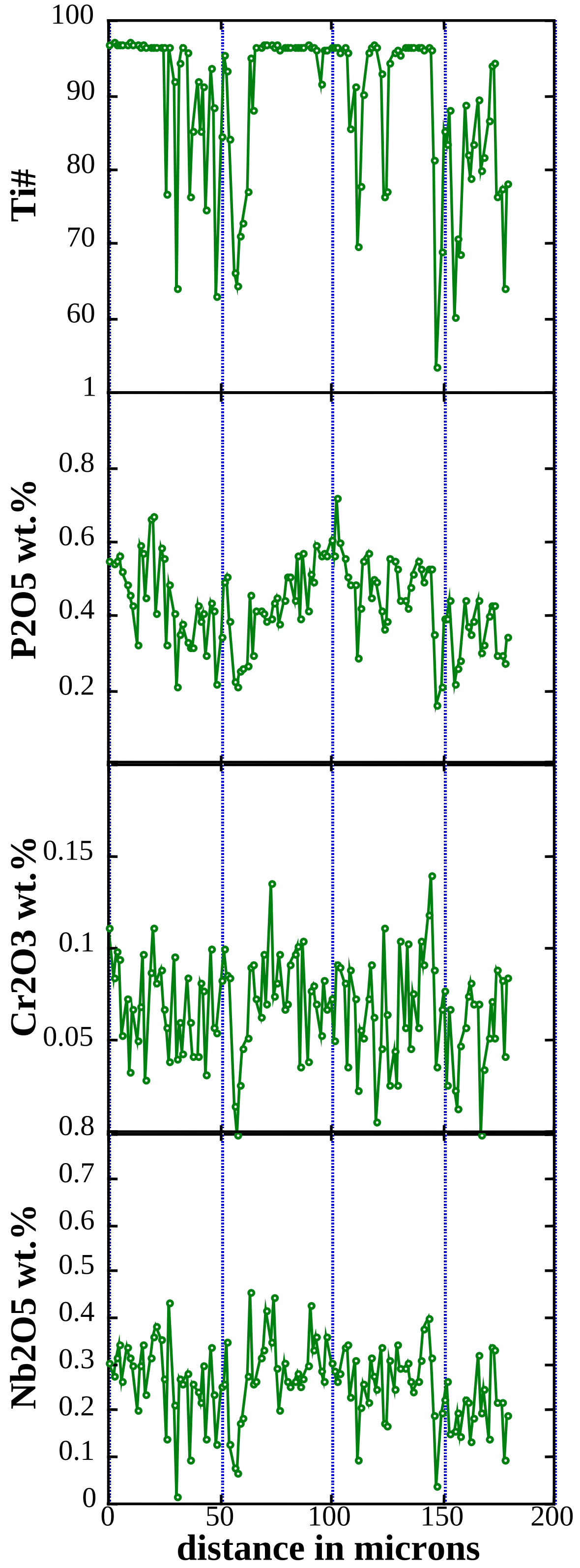

Figure 21b.

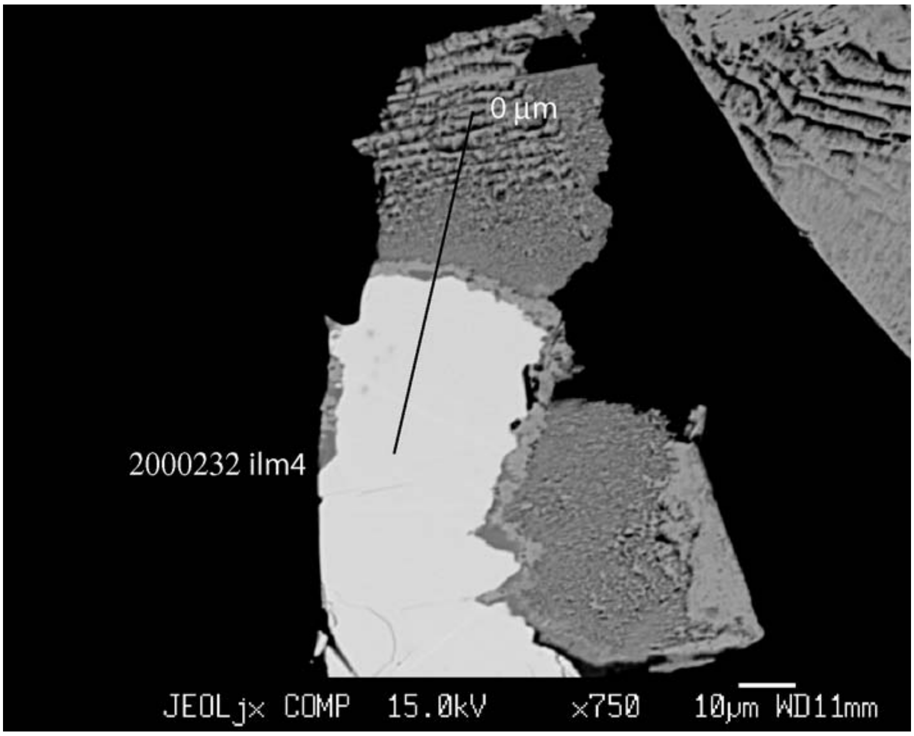

Figure 22. *Advanced alteration of ilmenite, sample 2000232.*

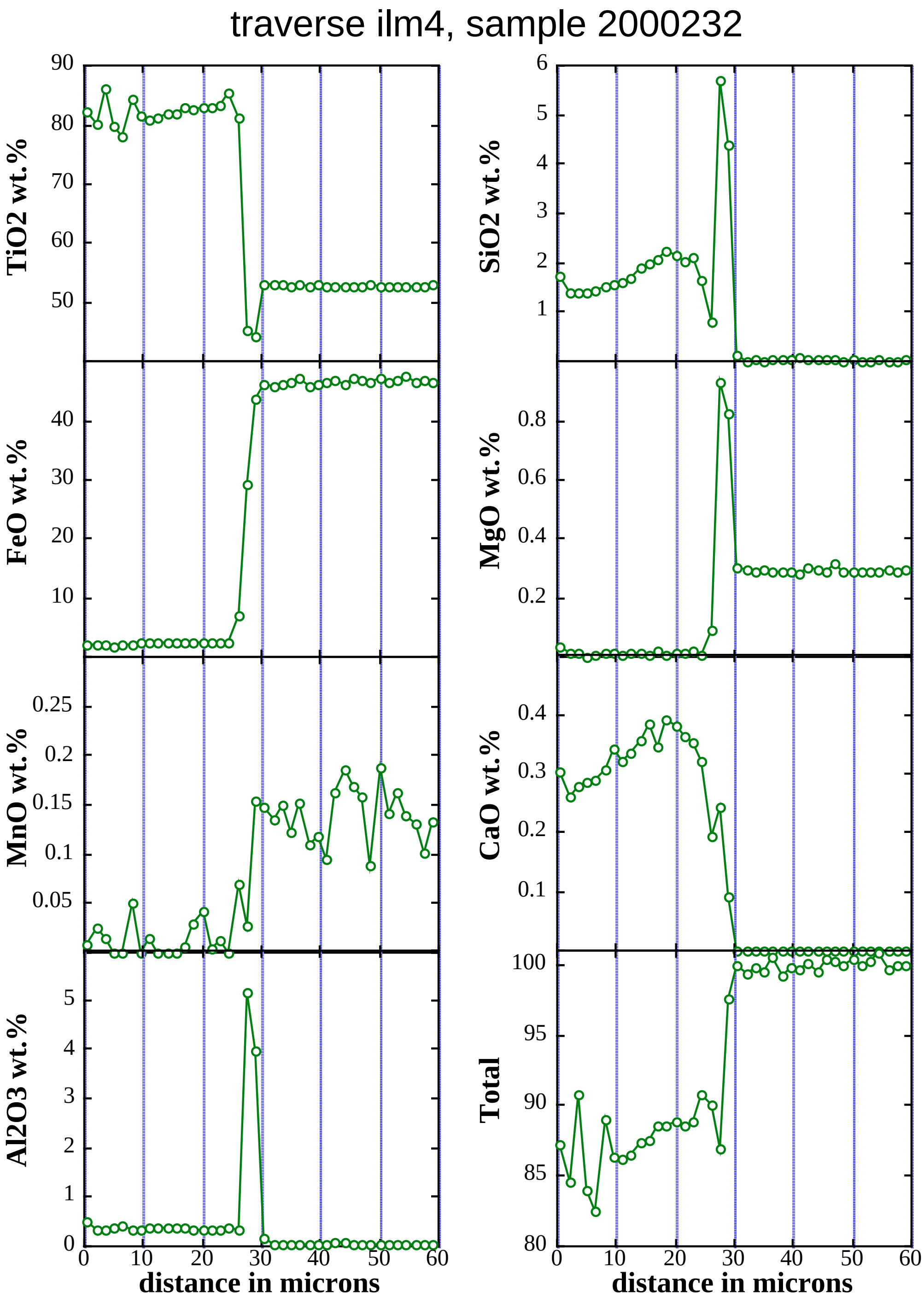
traverse ilm4, sample 2000232
TiO2 wt.%
SiO2 wt.%
FeO wt.%
MgO wt.%
MnO wt.%
CaO wt.%
Al2O3 wt.%
Total
distance in microns
distance in microns

Figure 23a.

traverse ilm4, sample 2000232

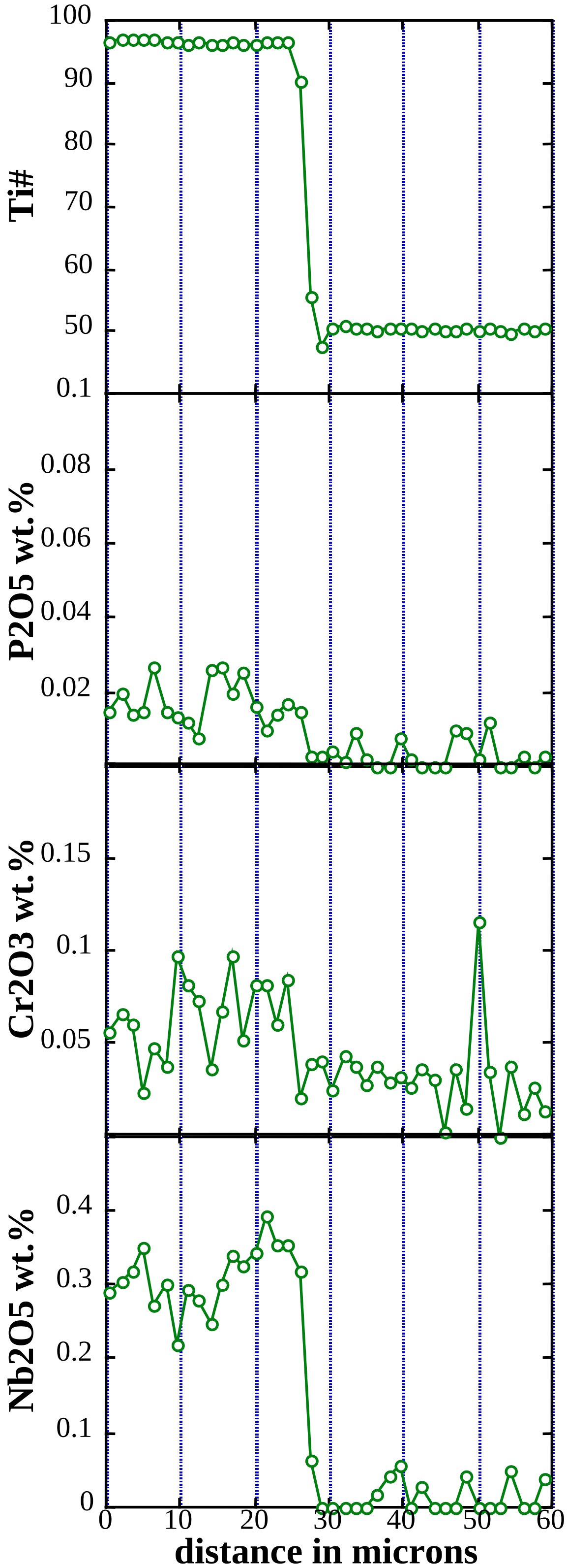

Figure 23b.

Ilm4 grain is probably a fragment of a larger ilmenite grain. The analysed grain has unaltered ilmenite at one end (Fig. 22). The traverse runs from within the altered ilmenite into the unaltered part of the grain. Element concentrations for the two grain portions are nearly constant for TiO_2, FeO, Al_2O_3, SiO_2, MgO, and CaO (Fig. 23). The altered grain portion has high TiO_2 (>80 wt.%), low FeO, MnO, elevated Al_2O_3 (to 0.4 wt. %), high SiO_2 at 1.5 to 2 wt. %, very low MgO, and intermediate CaO at around 0.3 wt.%. P_2O_5 is very low for both altered and unaltered grain portion, but slightly elevated in the altered part. Nb_2O_5 is significantly higher in the altered part, with around 0.3 wt.%. Analytical total is less than 90 % compared to around 100 % for unaltered ilmenite.

Sample 2000237 - garnetiferous diorite (khondalite belt)

Two ilmenite grains were analysed in this sample. Ilmenite ilm1 is a ca. 100 μm x 300 μm grain, with patchy alteration to 20 μm from the grain rims (Fig. 24). The traverse ilm1 runs from one alteration patch across a portion of unaltered ilmenite and some 15 μm into another alteration patch. The unaltered ilmenite has about 51 wt.% TiO_2 and low Mn and Mg (both around 0.1 wt. % oxide) (Fig. 25). At the edge to the alteration patches, MnO increases to above 1 wt. %, and then drops to a level similar to the unaltered ilmenite, while TiO_2 increases to above 60 wt. % accompanied by significant increases in Al, Si, Mg, Ca, P, and Nb. Fe and analytical total show strong negative correlation with Ti in the alteration zones. Chromium is low throughout (< 0.1 wt. % Cr_2O_3).

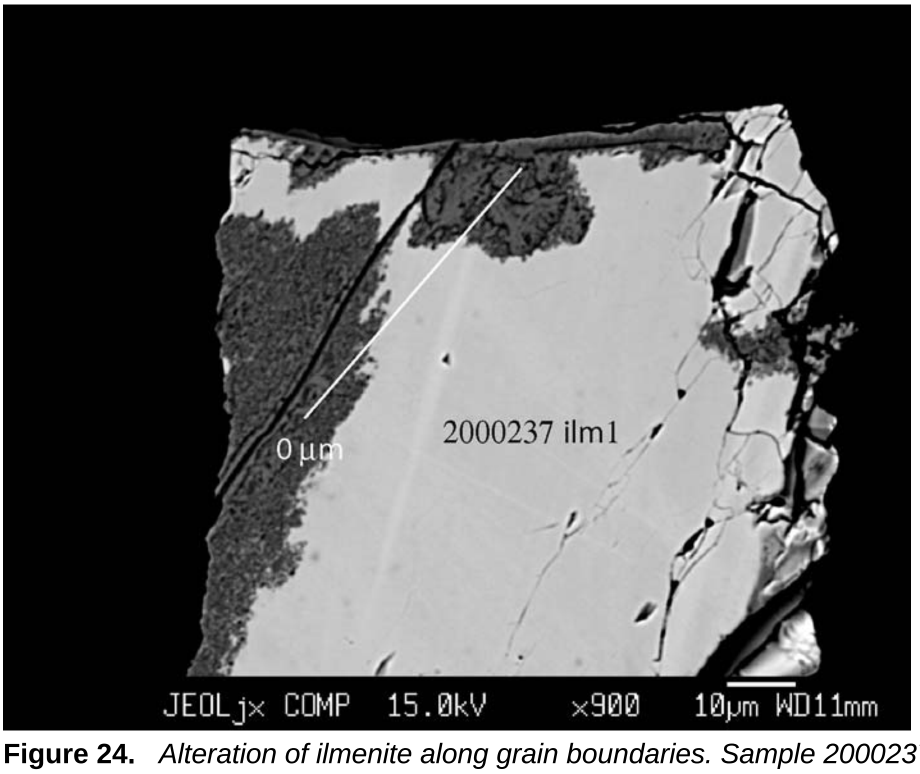

Figure 24. *Alteration of ilmenite along grain boundaries. Sample 2000237.*

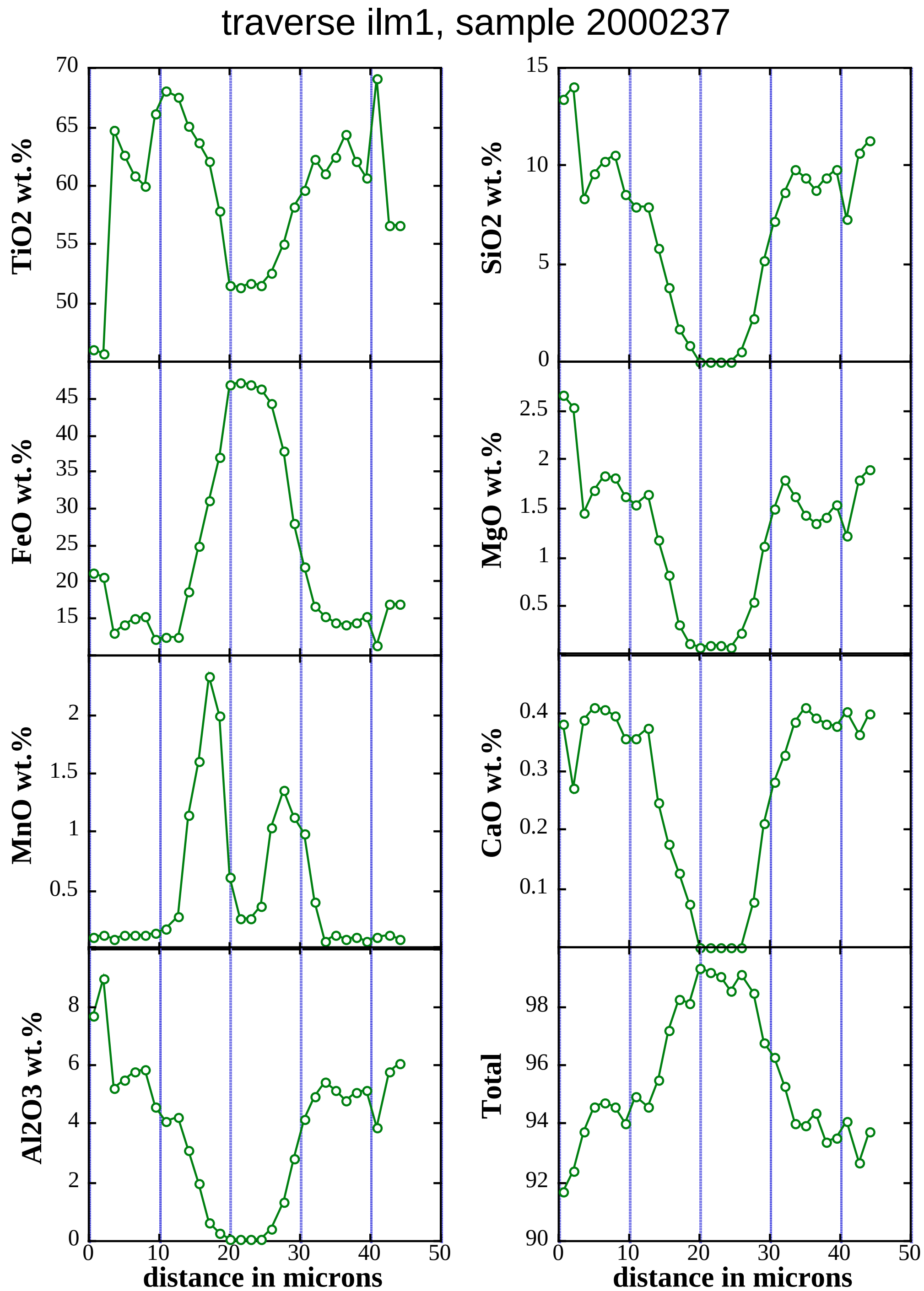

traverse ilm1, sample 2000237
TiO2 wt.%
SiO2 wt.%
FeO wt.%
MgO wt.%
MnO wt.%
CaO wt.%
Al2O3 wt.%
Total
distance in microns
distance in microns

Figure 25a.

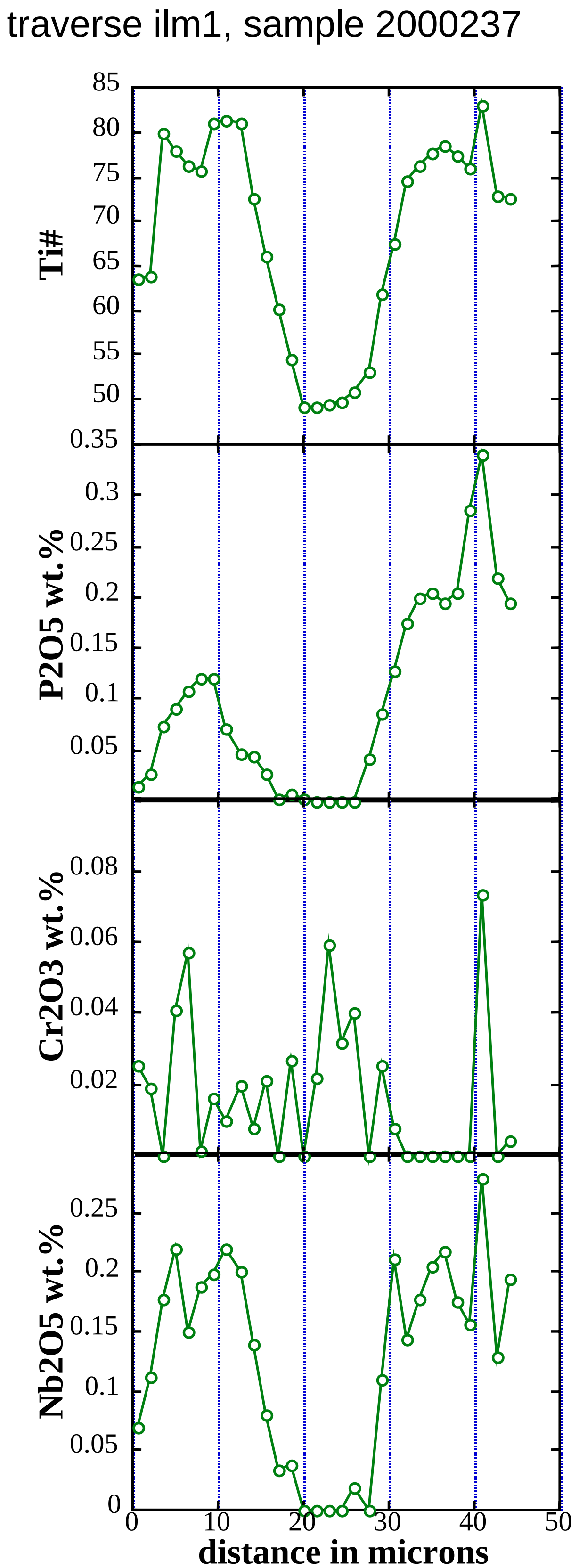
traverse ilm1, sample 2000237
Ti#
P2O5 wt. %
Cr2O3 wt. %
Nb2O5 wt. %
distance in microns
85
80
75
70
65
60
55
50
0.35
0.3
0.25
0.2
0.15
0.1
0.05
0.08
0.06
0.04
0.02
0.25
0.2
0.15
0.1
0.05
0
0
10
20
30
40
50

Figure 25b.

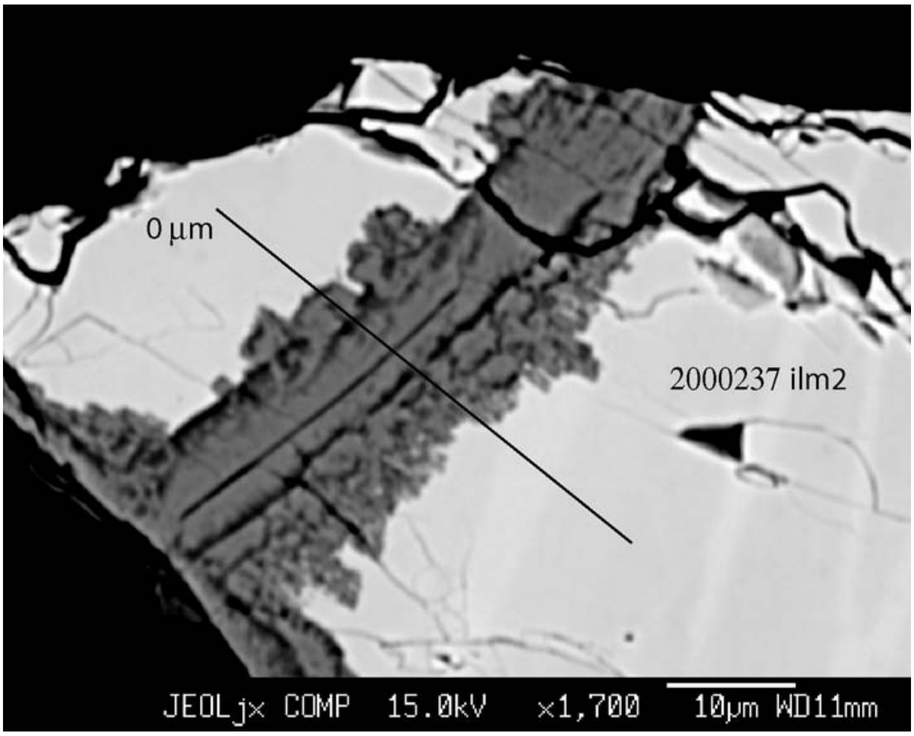

Figure 26. *Alteration of ilmenite along fracture. Sample 2000237.*

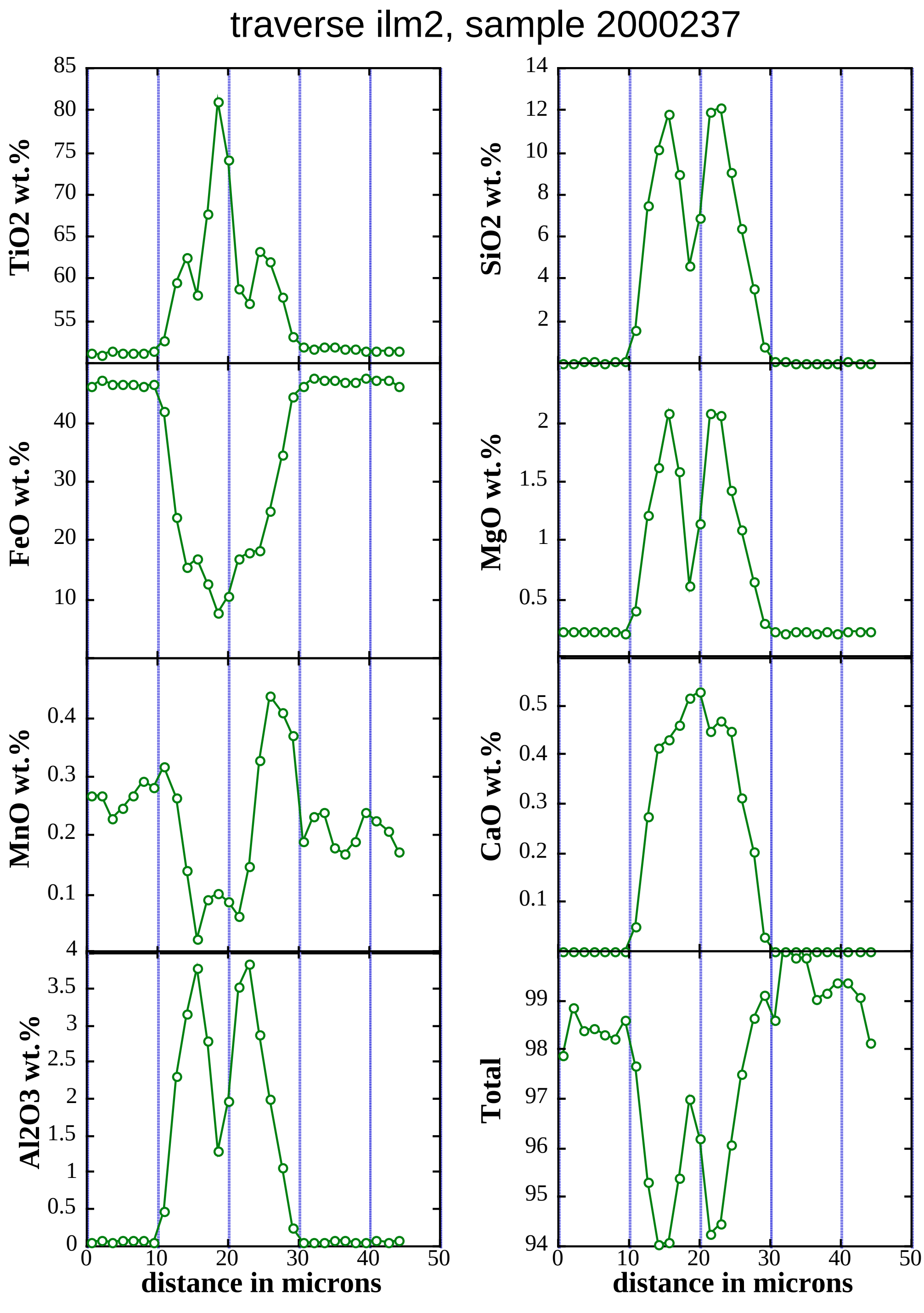
traverse ilm2, sample 2000237
TiO2 wt.%
SiO2 wt.%
FeO wt.%
MgO wt.%
MnO wt.%
CaO wt.%
Al2O3 wt.%
Total
distance in microns
distance in microns

Figure 27a.

traverse ilm2, sample 2000237

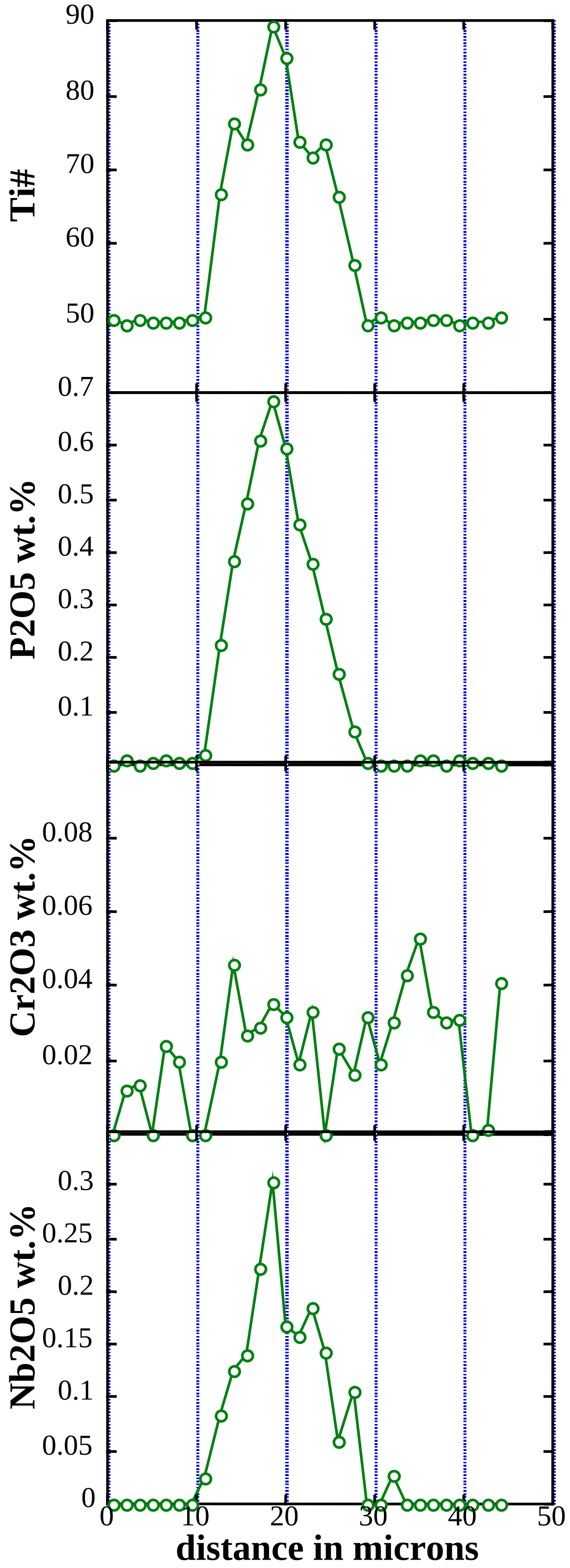

Figure 27b.

Ilmenite ilm2 is a 70 μm x 120 μm grain, where the alteration is developed parallel to a fracture (Fig. 26). The traverse ilm2 runs across this fracture from and to unaltered areas of the ilmenite grain. Elemental variation along the traverse (Fig. 27) shows a high degree of parallelism across the fracture. The unaltered ilmenite has 51 wt. % TiO_2 and intermediate MnO of 0.25 wt. %, and low MgO of about 0.2 wt. %. All other elements apart from Fe show concentrations close to detection limit in the unaltered ilmenite areas. At the edge of the alteration domains, TiO_2 increases rapidly to about 60 wt. %, and then shows a peak at about 80 wt. % in the center of the alteration fracture. The Mn starts with a significant increase, although much smaller than in grain ilm1 (to >0.4 wt. % MnO), but then drops to very low contents (<0.1 wt% MnO) in the centre of the fracture. Similar patterns are seen for Al_2O_3, SiO_2, and MgO which all starts showing a positive correlation with TiO_2, but then shows a negative correlation as the high TiO_2 centre of the fracture is reached. CaO, P_2O_5 and Nb_2O_5 are anomalous in this respect, since they all continue to increase into the centre of the fracture, and FeO shows a constant negative correlation.

Sample 2000256 - garnet-orthopyroxene gneiss (khondalite belt)

Two ilmenite grains were analysed in this sample. Ilmenite ilm1 is a 100 x 120 μm grain, with alteration halos around fractures (Fig. 28). The traverse runs across the alteration from the unaltered ilmenite. The unaltered ilmenite grain has TiO_2 around 51 wt. % and intermediate MnO of 0.3 wt. % and low MgO at about 0.15 wt.% (Fig. 29). Al, Si, Ca, P, Cr, and Nb are all at detection limits. The alteration halo is symmetric around the fracture, with shoulders of high TiO_2 (to 70 wt.%) dropping somewhat to about 65 wt.% in the centre. MnO shows a subtle increase from 0.3 to 0.35 wt.% at the shoulder, and then displays a negative correlation with TiO_2. A similar relationship is seen with MgO, SiO_2, Al_2O_3, and FeO while P_2O_5 and Nb_2O_5 are nearly constant and high within the alteration halo.

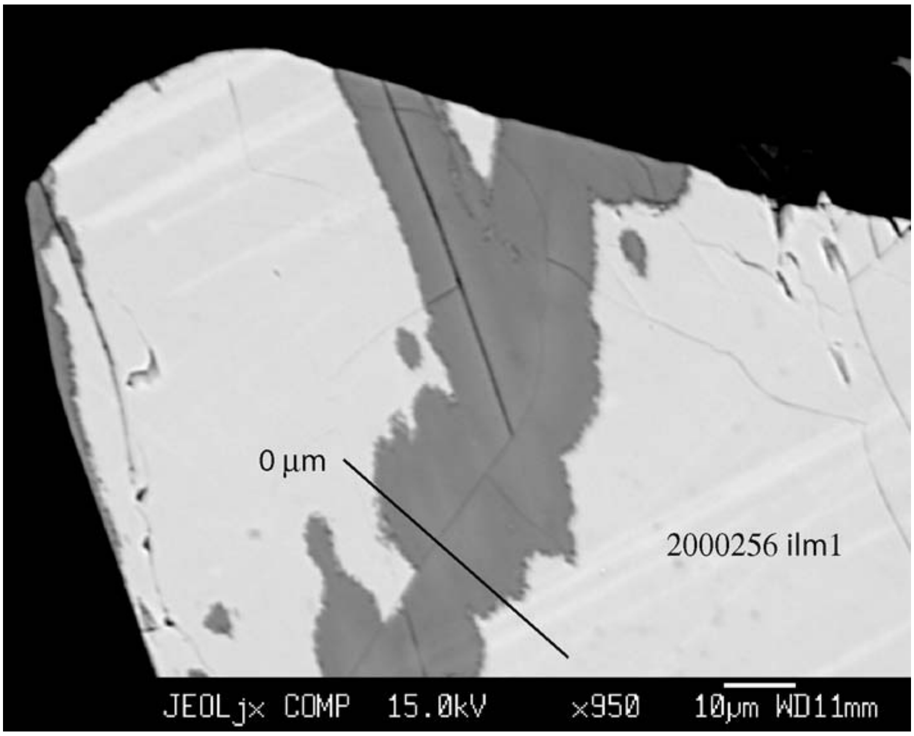

Figure 28. *Alteration of ilmenite along fracture. Sample 2000256.*

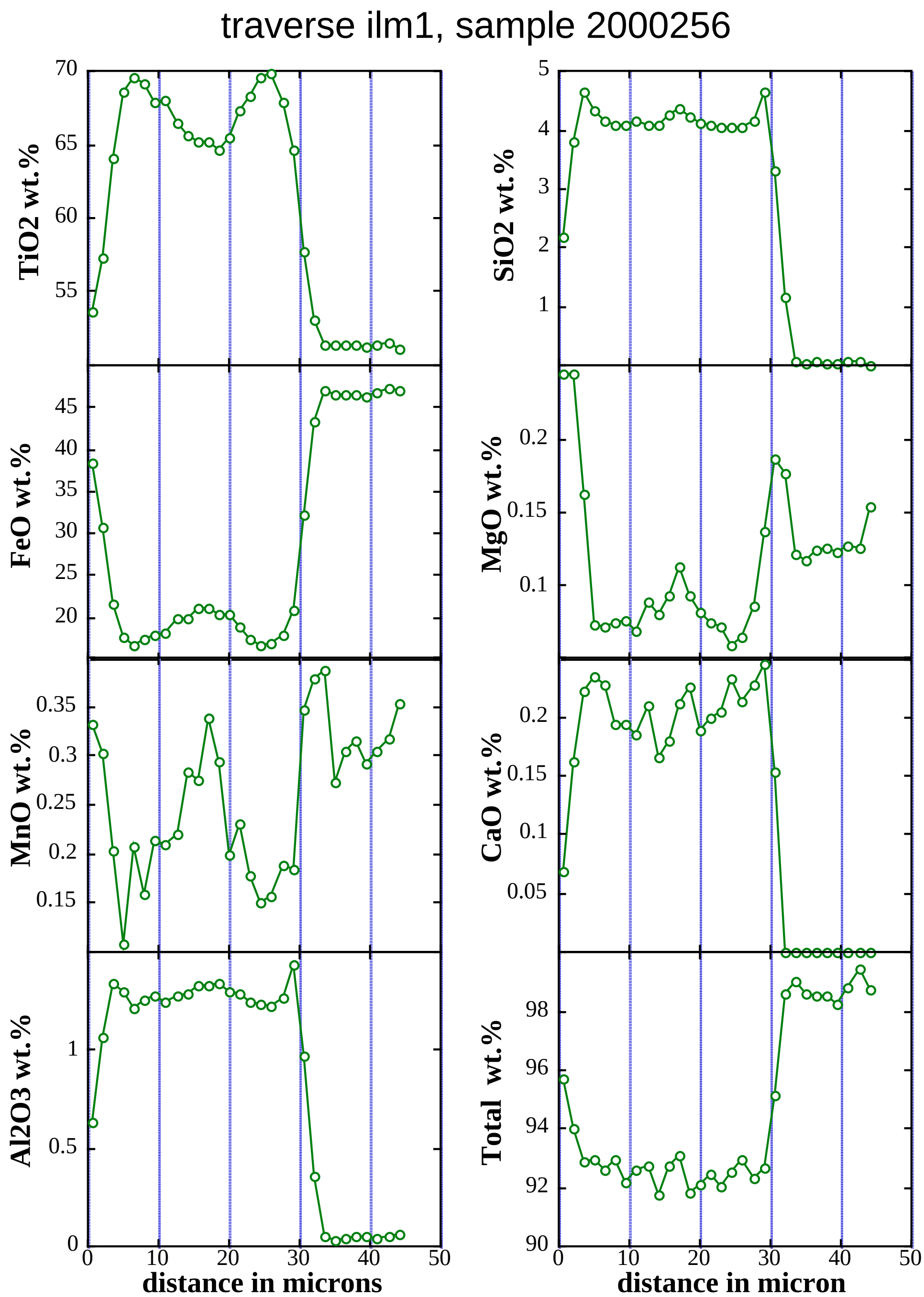
traverse ilm1, sample 2000256
TiO2 wt.%
SiO2 wt.%
FeO wt.%
MgO wt.%
MnO wt.%
CaO wt.%
Al2O3 wt.%
Total wt.%
distance in microns
distance in micron

Figure 29a.

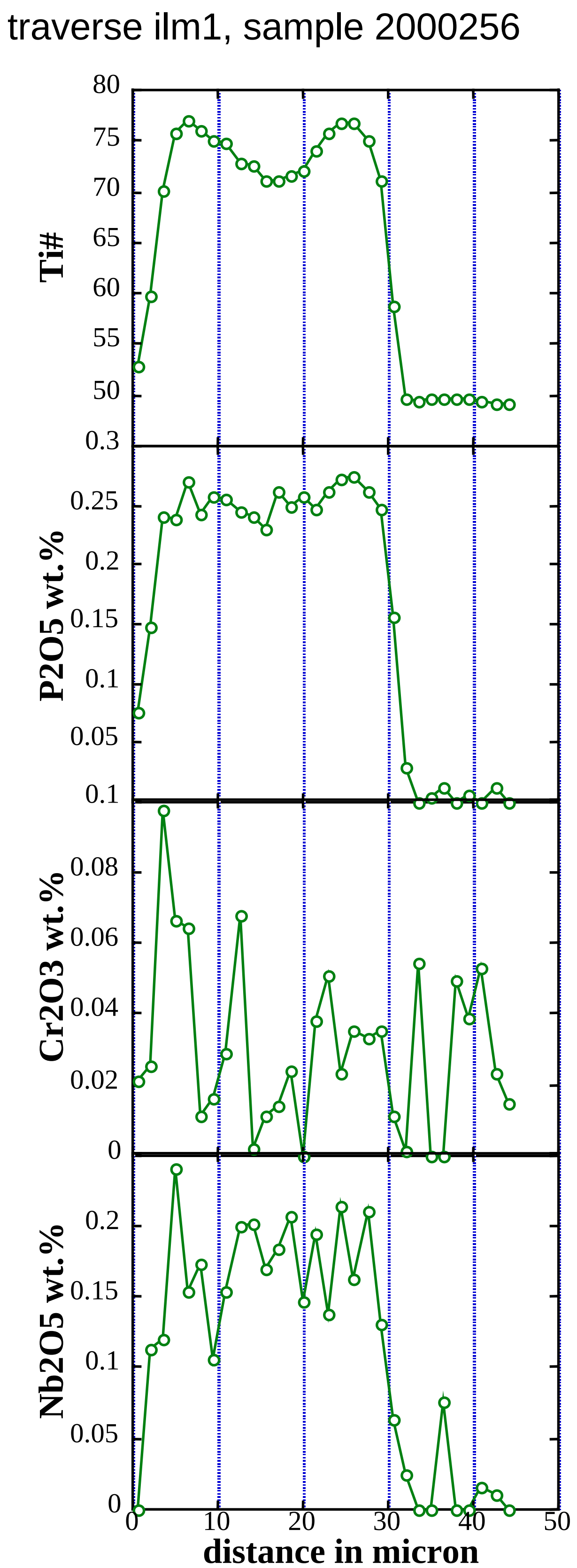
traverse ilm1, sample 2000256
Ti#
80
75
70
65
60
55
50
P2O5 wt.%
0.3
0.25
0.2
0.15
0.1
0.05
Cr2O3 wt.%
0.1
0.08
0.06
0.04
0.02
0
Nb2O5 wt.%
0.2
0.15
0.1
0.05
0
0
10
20
30
40
50
distance in micron

Figure 29b.

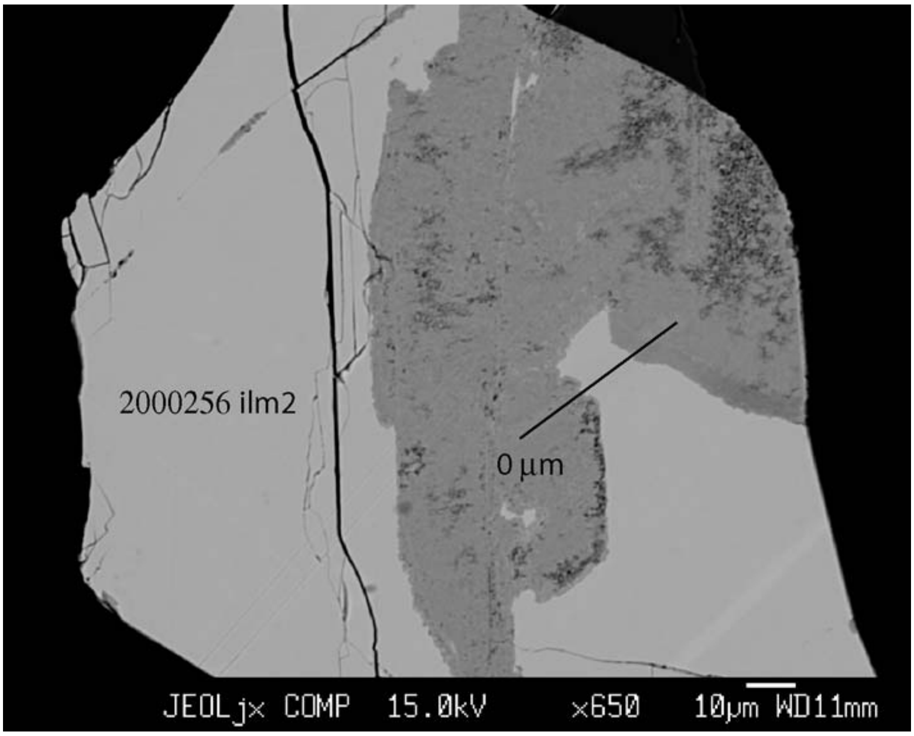

Figure 30. *Altered ilmenite grain. The alteration is perhaps following a fracture, but this is not as clear as on the examples in e. g. Fig 28. The prominent fracture in the left part of the grain is probably introduced during the mechanical treatment of the sample prior to heavy mineral separation. Sample 2000256.*

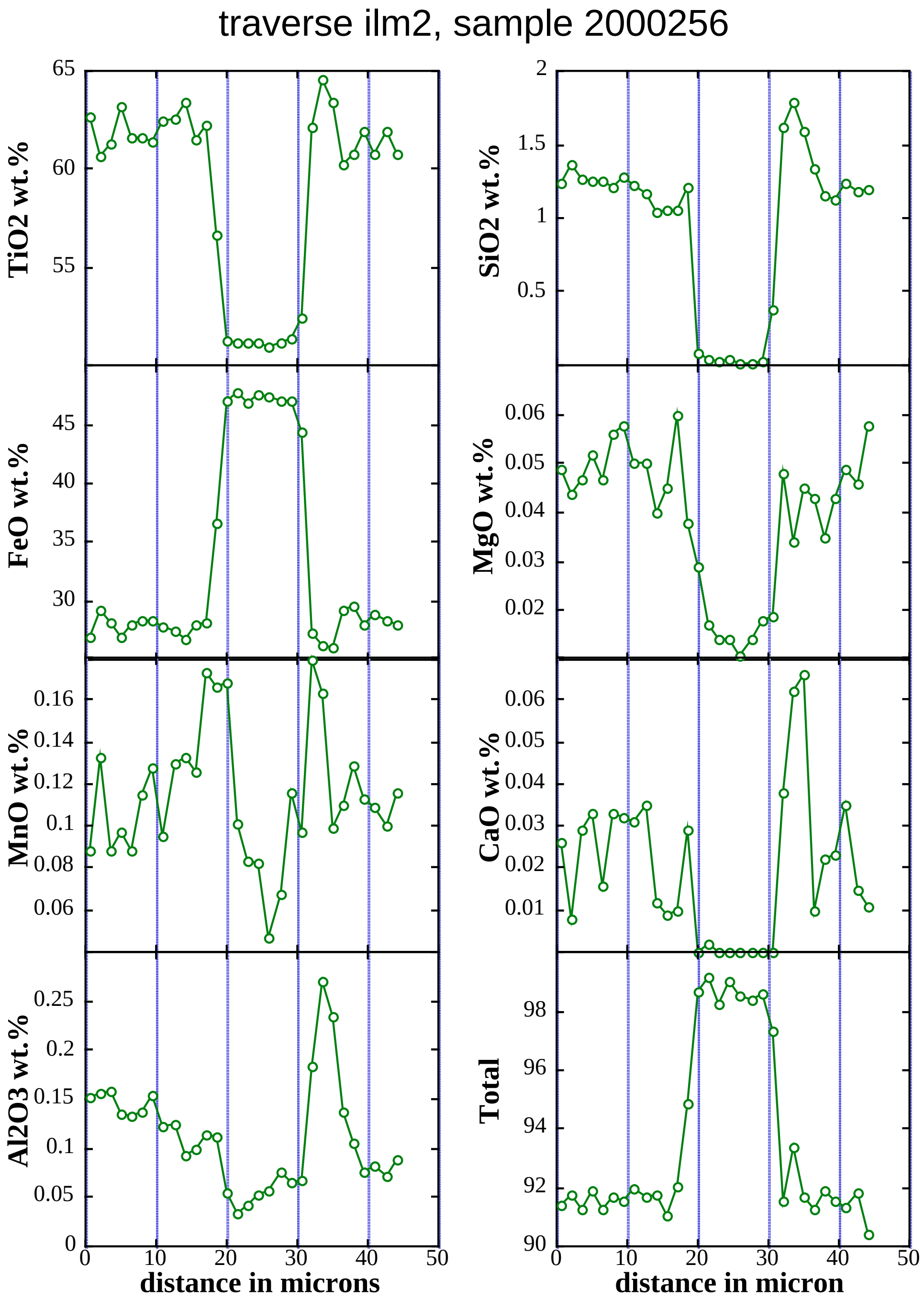
traverse ilm2, sample 2000256
TiO2 wt.%
SiO2 wt.%
FeO wt.%
MgO wt.%
MnO wt.%
CaO wt.%
Al2O3 wt.%
Total
distance in microns
distance in micron

Figure 31a.

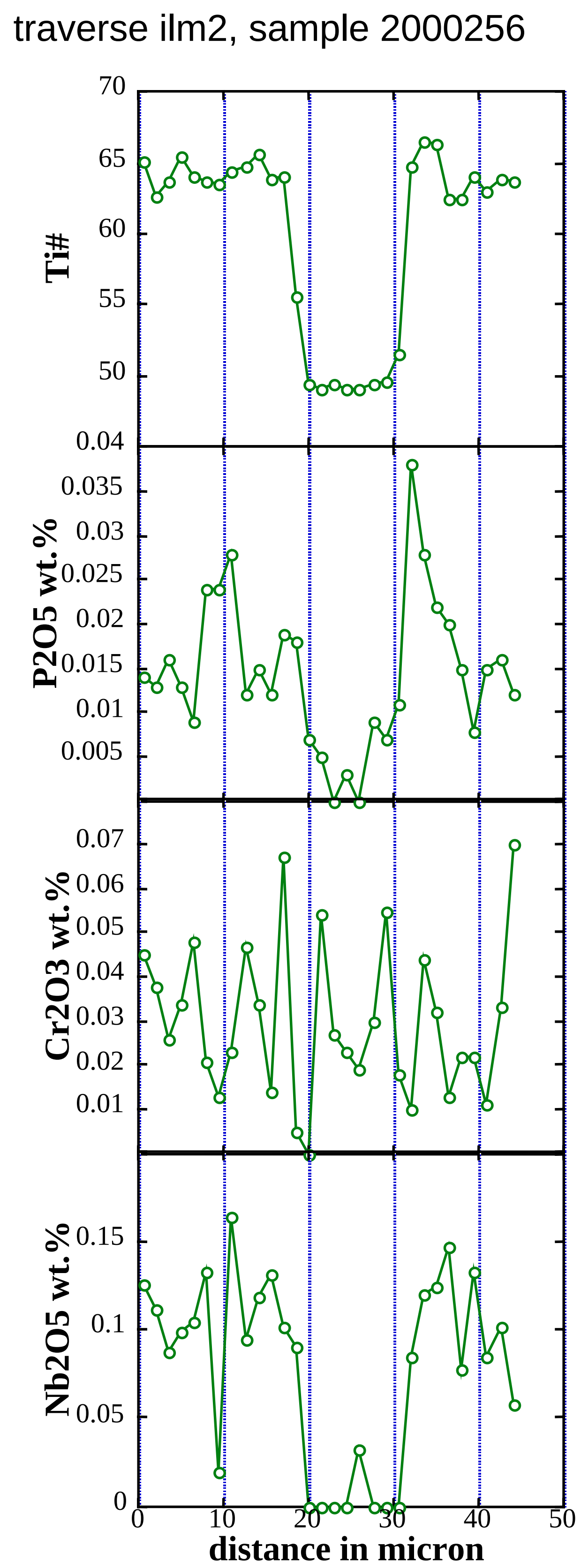
traverse ilm2, sample 2000256
Ti#
P2O5 wt.%
Cr2O3 wt.%
Nb2O5 wt.%
distance in micron
0
10
20
30
40
50

Figure 31b.

Ilmenite ilm2 displays a large alteration patch, which appears to be following crystallographic planes (Fig. 30). The traverse starts within the altered patch, and runs across the unaltered ilmenite. Similar to ilm1, the unaltered ilm2 grain shows TiO_2 of about 51 wt. % and very low MnO, MgO, SiO_2, Al_2O_3, P_2O_5, Cr_2O_3 and Nb_2O_5, which all are close to detection limit (Fig. 31). At the edge of the alteration zones, where TiO_2 jumps to a rather steady 61-63 wt. %, MnO jumps to nearly 0.2 wt. % and then drops to about 0.1 wt. %. The alteration zones are further characterized by having low FeO (<30 wt. %), elevated Al_2O_3, SiO_2, MgO, CaO, P_2O_5, and Nb_2O_5 compared to the unaltered ilmenite. Analytical total is low, at around 92 wt. %.

Sample 2000259 - two-pyroxene gneiss (khondalite belt)

The analysed grain is euhedral and about 100 μm in the long dimension (Fig. 32). This grain shows alteration along one side, which is characterised by a spongy appearence, but in places separated by smaller volumes of more homogeneous material. The start of the traverse shows a uniform distribution of elements, with very low concentrations of all trace elements, except MnO and MgO of about 0.5 wt. % (Fig. 33). The homogeneous (grey in Fig. 32) area has elevated TiO_2 to about 75 wt. % with an increase of the oxides of Si, Al, Ca and Nb, and a decrease in the oxides of Fe, Mn and Mg. The spongy alteration zone shows an inverse relationship between TiO_2, which increases to nearly 90 wt. %, and the elements Fe, Mn, Al, Si, Mg and to some extend Ca, which is only enriced in a light grey area around 18 microns.

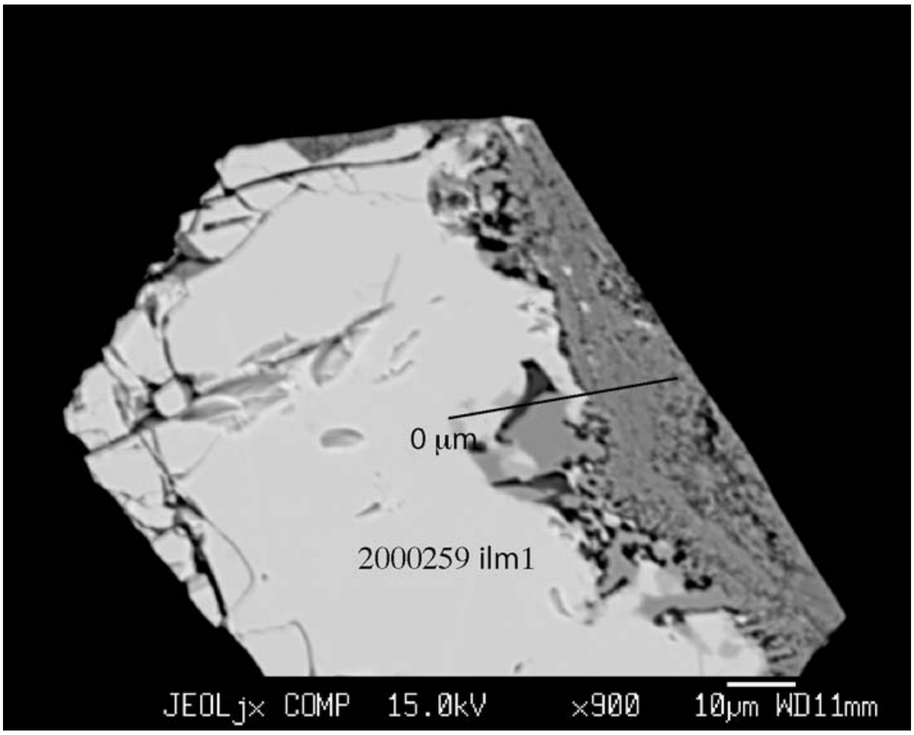

Figure 32. *Complex alteration patterns along grain boundary. Sample 2000259.*

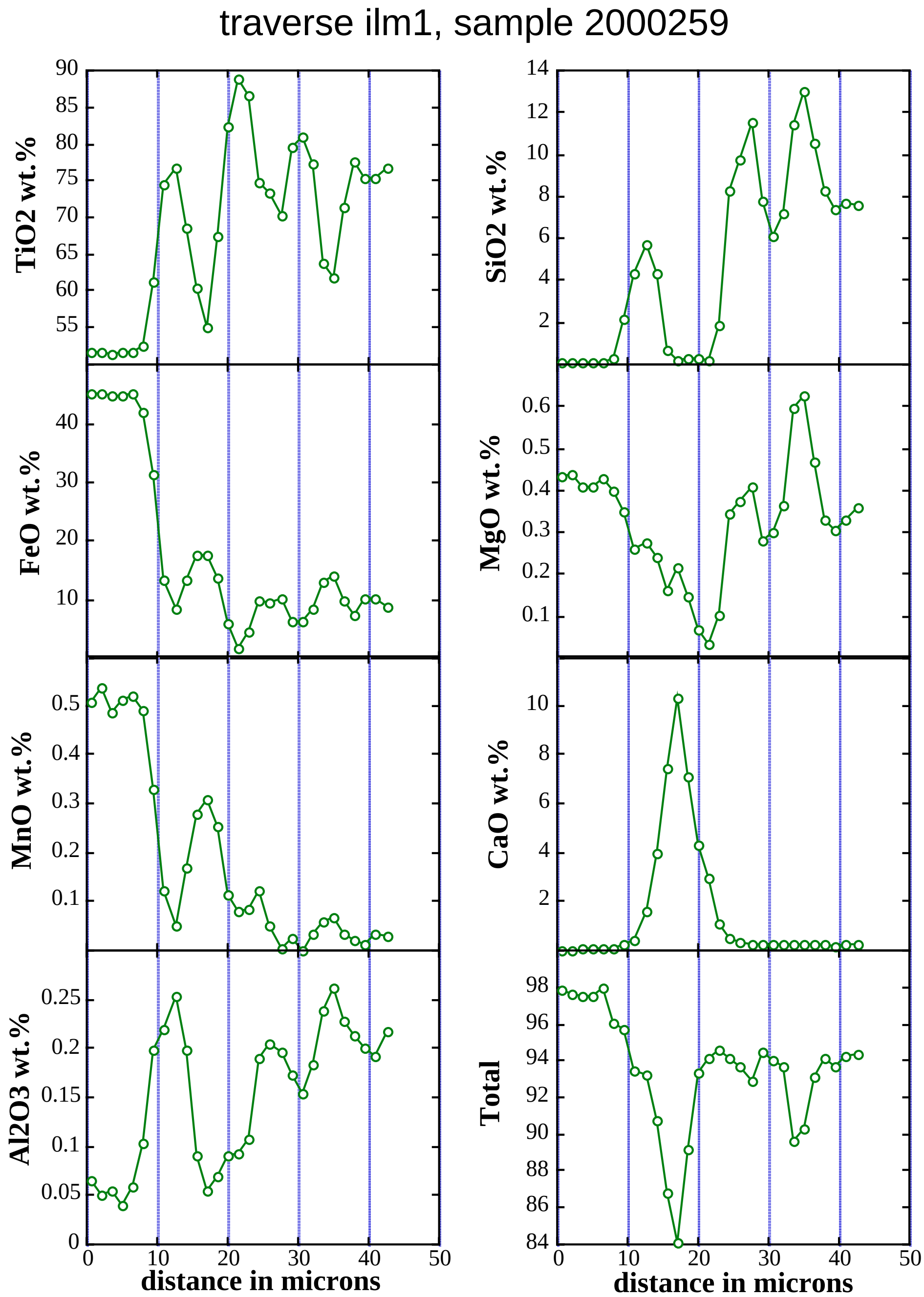

traverse ilm1, sample 2000259
TiO2 wt.%
SiO2 wt.%
FeO wt.%
MgO wt.%
MnO wt.%
CaO wt.%
Al2O3 wt.%
Total
distance in microns
distance in microns

Figure 33a.

traverse ilm1, sample 2000259

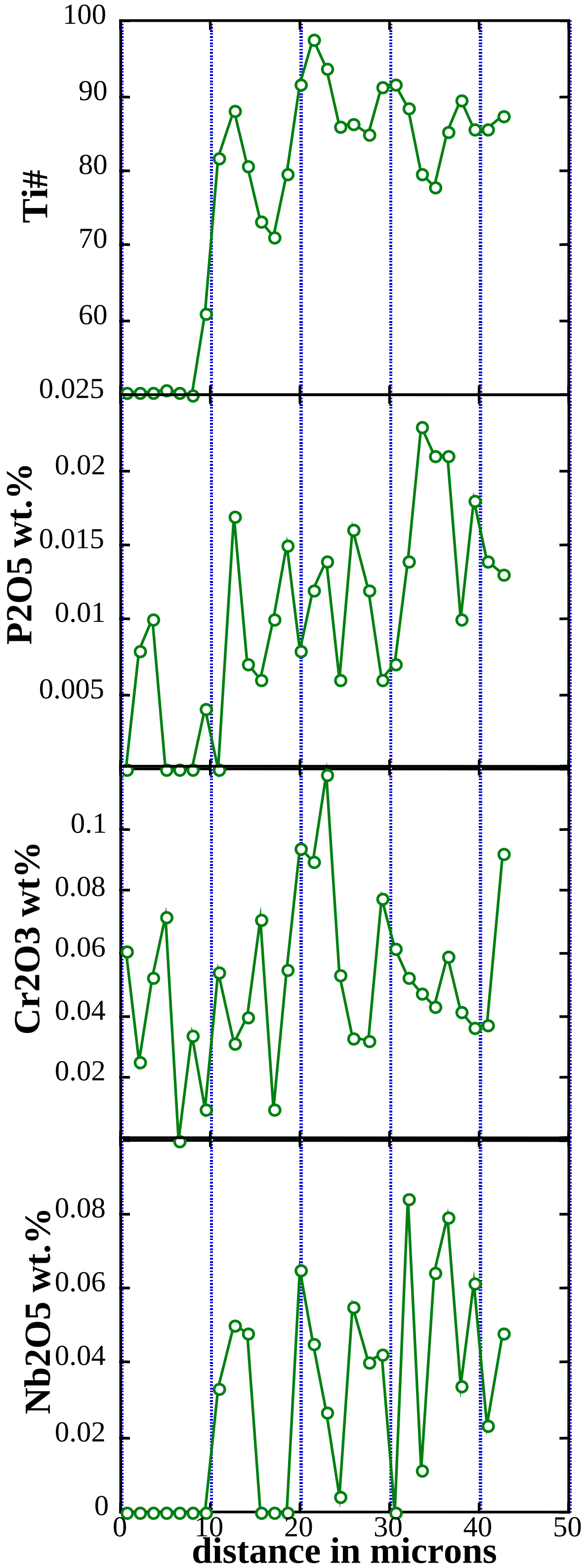

Figure 33b.

8. Discussion

8.1 Alteration of ilmenite to pseudorutile or hydroxy-pseudorutile

Studies on the alteration of ilmenite (Ti/(Ti+Fe)*100 = Ti# = 50; Table 2), shows that the process passes through several stages (see e. g. Grey & Reid (1975); Frost et al., 1983). The first is the anodic reaction of Fe oxydation of the Fe2+ in ilmenite to form a ferri-ilmenite, which subsequently goes through an hydrooxylation and formation of a goethite component ($Fe(OH)_3$) which is easily dissolved and removed. This leaves a $Fe_2Ti_3O_9$ compound, pseudorutile, often showing epitaxial overgrowth on the replaced ilmenite. Pseudorutile has a Ti# of 60. Because of the volume reduction, which is in the order of 6-10 %, the pseudorutile will be heavily cracked and pitted. This in turn favours the infiltration of reacting hydrous agents to further induce hydrooxylation and leaching of iron from the pseudorutile to form a hydrated pseudorutile by the reaction $Fe_2Ti_3O_9$ + $0.75H_2O$ to $Fe_{1.5}Ti_3O_{7.5}(OH)_{1.5}$ + 0.5 $FeO_{1.5}$ (hematite). $Fe_{1.5}Ti_3O_{7.5}(OH)_{1.5}$ has Ti# of 66.7. This reaction can proceed to form a series of hydroxylian pseudorutile of the form $Fe_{0.67}Ti_3O_5(OH)_4$ (Ti# = 82) or $Fe_{0.33}Ti_3O_5(OH)_3$ (Ti# = 90) (Grey et al., 1994). Further leaching of iron results in the formation of recrystallized anatase or rutile TiO_2, which will have a Ti# of 100. In short, the progressive alteration and leaching of ilmenite will therefore pass through four stages:

pseudorutile $Fe_2Ti_3O_9$ (Ti# 60) or hydroxy-pseudorulite $Fe_{1.5}Ti_3O_{7.5}(OH)_{1.5}$ (Ti# 67)
hydroxy-pseudorutile $Fe_{0.67}Ti_3O_5(OH)_4$ (Ti# 82)
hydroxy-pseudorutile $Fe_{0.33}Ti_3O_5(OH)_3$ (Ti# 90)
rutile (anatase) TiO_2 (Ti# 100)

Table 2. ***Ideal composition of ilmenite and alteration products***

		TiO_2	Fe_2O_3	FeO	Total	Ti#
ilmenite	$FeTiO_3$	52.70	-	47.30	100.00	50
pseudorutile	$Fe_2Ti_3O_9$	60.02	39.98	-	95.99	60
hydroxy-pseudorutile	$Fe_3Ti_6O_{15}(OH)_3$	62.27	31.11	-	90.26	67
hydroxy-pseudorutile	$Fe_{0.67}Ti_3O_5(OH)_4$	66.36	14.81	-	79.69	82
hydroxy-pseudorutile	$Fe_{0.33}Ti_3O_5(OH)_3$	75.54	8.39	-	83.09	90
hydroxy-rutile (?)	$Ti_3O_5(OH)_2$	87.58	-	-	87.58	100
rutile	TiO_2	100.00	.00	.00	100.00	100

Ti#=100*Ti/(Ti+Fe)

Several of these alteration stages have been found in the altered ilmenite grains presented above, and in the following will be presented some examples:

a) One typical example of alteration of ilmenite to pseudorutile is seen in ilm1 grain from sample 2000224 (Fig. 14). Over an alteration front of some 10 μm, this manganese-rich ilmenite grain is altered to a pitted and cracked material (Fig. 15), with about 60 wt. TiO_2, and ca. 28 wt % FeO, of which all probably is present as Fe3+. The Ti# jumps from 50 in unaltered ilmenite to around 60 for the pseudorutile Adding the 4 wt % MnO, it brings the total FeO+MnO to about 32 wt. %. From Table 2, it is seen that this corresponds closely to pure pseudorutile, which has 60 wt % TiO_2 and 36 wt. % FeO. The total for pure pseudorutile is 96 wt. %, which allows for the extra oxygen in the Fe3+ component, and this compares well with the 94 wt. % total for the altered grain in 2000224 ilm1. The increase in MnO across the alteration front is also typical for the general alteration of ilmenite, because of the lower oxydation potential for manganese compared to iron - i.e. iron is oxydized first and leached away, followed by manganese, which accounts for the decrease in MnO at the formation of pseudorutile (see also Frost et al., 1986). MgO can be regarded as substituting for FeO in ilmenite and is leached away along with iron. Conversely, Al and Si show small, but significant increases, which can only be explained by the introduction of minute crystals of silicate minerals into the porous pseudorutile. In this case, the silicate impurities did not involve the introduction of Nb, Cr or P (Fig. 15).

b) A similar case of ilmenite alteration, but which is slightly more complex is found in the ilm1 grain in sample 2000237 (Figs. 24 and 25). In this grain, the central, unaltered ilmenite has only 0.3 wt. % MnO, but shows a sharp increase over the alteration fronts of ca. 10 μm to 1-2 wt. % MnO, whereafter it falls to very low levels. FeO drops to a level of ca. 13 wt. %, while TiO_2 reaches about 68 wt. %. The Ti# in the altered ilmenite is around 80. This corresponds to a hydroxy-pseudorutile of the form $Fe_{0.67}Ti_3O_5(OH)_4$ (Table 2) which has 66.4 wt. % TiO_2 and 13.3 wt. % FeO, giving a total of 79.7 wt. %, and with Ti# of 82. The analytical total in the high TiO_2 regions of the altered ilm1 grain has about 94 wt. % total, but this includes rather high SiO_2, Al_2O_3, and MgO plus CaO, P_2O_5 and Nb_2O_5, which add up to some 14 wt. %. These elements must have been introduced after or during the alteration process, and probably represent silicate impurities.

c) Grain ilm2 from sample 2000237 shows alteration along a preexisting fracture in the ilmenite (Figs. 26 and 27). The edges of the alteration halo again shows an increase in MnO over ca. 10 μm, but to values of only 0.4 wt. % MnO. The Ti# increases through an intermediate level of about 70-75 to a peak of 90 in the axial part of the altered ilmenite. This corresponds to hydroxy-pseudorutile of the most leached form $Fe_{0.33}Ti_3O_5(OH)_3$ (Table 2). Due to the three hydroxygroups, the total of this hydroxy-pseudorutile is around 83 wt. %, and the higher analytical totals for the altered parts of ilm2 is due to the significant impurities of Al, Si, Mg, and Ca. Also, the levels of phosphorous and niobium are high. It is of some interest to note that while the levels of Al, Si, and Mg decreases with the formation of $Fe_{0.33}Ti_3O_5(OH)_3$, contrations of Ca, P, and Nb continue to increase. This suggests that the progressive leaching of pseudorutile leads to recrystallization and removal of the silicate impurities, while Nb is incorporated into the pseudorutile, perhaps due to the incipient formation of anatase. The coupled increase in P and Ca on the other hand points to crystallization of apatite. The apparent constant level of Ca and P over the altered part of the grain suggests that apatite, once formed, stays as impurities in the hydroxy-pseudorutile, and is left untouched by

d) Examples of alteration of ilmenite to material dominated by Ti-rich phases, perhaps anatase, is found in the grains ilm3 and ilm4 in sample 2000232. The large grain ilm3, rep resents completely altered ilmenite (Fig. 20). Most of the analysed elements vary greatly in concentrations, as described above (Fig. 21). The grain is very porous and shows domains of high Ti# of about 97, with intermittent areas of varying, but mostly lower Ti# values. These lower Ti# areas are also much higher in Si, Al, Fe, and Mg, and slightly lower in Nb. CaO and P_2O_5 appear constant along the traverse, and the interpretation is therefore similar to that of grain ilm2 from sample 2000237 presented above, that the Si, Al, Fe, and Mg represents silicate impurities which are leached away as the Ti-rich phase gradually crystallizes. The constant CaO and P_2O_5 probably represents apatite impurities which are resistant to the progressive leaching. The other grain ilm4 (Figs. 22 and 23) contains a core of unaltered ilmenite. Both grains are illustrated in Fig. 20, and the altered grains show the same textures with porosities arranged in what appears to be subparallel planes. The altered part of ilm4 shows a constant Ti# of 97 and the concentration of other elements is low, similar to the highest Ti# portions of ilm3. One exception is the behavior of CaO which correlates with SiO_2, and is much higher than P_2O_5, which is at a constant and very low concentration level. Apparently apatite did not form during the alteration of this ilmenite grain, and calcium likely is part of the silicate impurities.

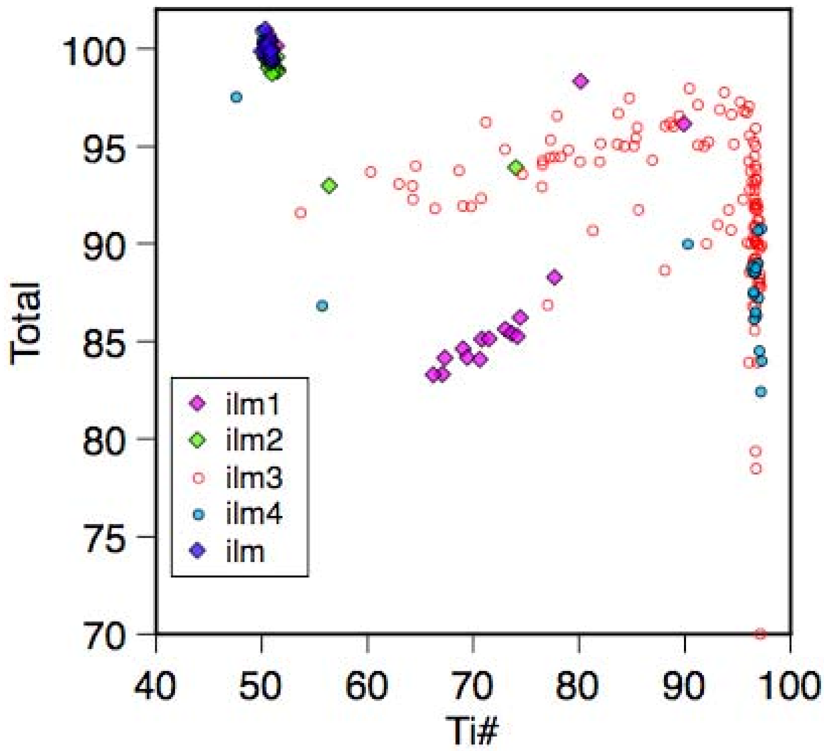

Figure 34. *Electron micro-probe data of the four altered ilmenite grains, and some unaltered ilmenite grains (blue diamonds). The total is given in wt. %.*

One matter of question in the alteration product of these two grains, is the nature of the Ti-rich phase(s). From the constant Ti# of 97, it is clear that the phase has been leached beyond the hydroxy-pseudorutile $Fe_{0.33}Ti_3O_5(OH)_3$, which has a Ti# of 90 (Table 2). The phase has about 2 wt. % iron expressed as FeO. It is possible that this iron resides in the silicate impurities, and in this case the phase is probably anatase. However, anatase should yield an analytical total of 100 wt. %, perhaps somewhat less, in case of the silicate impurities being hydrous mineral. Inspecting Fig. 34 shows that the analyses with Ti# of 97 yield a total of 97 wt. % or less. In fact, there are few analyses with a total of 97 wt. %, most are less than 95 wt. %. If this trend of constant Ti# with the analytical total varying between 97 and 85 is taken as a measure of impurities mixed into a TiO_2-rich material with Ti# of 97, the amount of hydroxy groups from these impurities can be estimated. Taking grain ilm4 as an example, the analytical total is between 85 and 90 wt. % for a constant Ti# of 97. The maximum amount of silicate impurities in these analyses are (FeO 2wt. %+ Al_2O_3 0.5 wt.% + SiO_2 2 wt. % + CaO 0.3 wt. %) = ca 5 wt. %. The maximum content of hydroxy groups in clay minerals amounjt to about 20 wt. % H_2O, which in this context would only account for about 1 wt. % of the analytical total (20 % of 5% = 1%). In other words, the material with

Ti# of 97 would appear to have an analytical total of about 90 wt. %. Since anatase, as stated above should yield 100 wt. % total, this phase is interpreted as representing hydroxy-pseudorutile, from which all or nearly all iron has been leached, and which is charge balanced only by 2 OH groups, with the formula $Ti_3O_5(OH)_2$. This iron-free hydroxy-pseudorutile would yield a total of 87.6 wt. % with a hypothetical Ti# of 100.

8.2 General styles of ilmenite alteration

Some general relationships can be extracted from this study. Two samples contain ilmenite grains showing alteration to iron-free hydroxy-pseudorutil with Ti# of 97, namely 2000232 (as presented above) and 2000259. For altered ilmenite from the other khondalite samples, the alteration products represent hydroxy-pseudorutile at various stages of iron leaching. Impurities of silicates, perhaps clay minerals judged from the relatively high Al/Si ratios, are usually present too, but in very different and varying amounts. The only sample (2000224) from outside the khondalite belt, which contains altered ilmenite, shows a different style of ilmenite alteration. Firstly, the ilmenite grains show only sporadic signs of alteration, and the alteration product is the 'first stage' pseudorutile, with relatively low Ti# of around 60. All other samples, which come from khondalite lithologies, contain ilmenite with alteration products of Ti#>>60. Also, there is a tendency for the alteration profiles of khondalite ilmenites to show a more abrupt transition from unaltered ilmenite to hydrous-pseudorutile with high Ti#. This was also found by Hough (2003) in her study of ilmenite from the same lithologies, although the examples presented here are not conclusive, because some ilmenite in samples 2000237, 232 and 256 also show transitional alteration styles.

One common feature for all examined ilmenite grains, is that the alteration zones are localised at grain boundaries and grain edges, or along fractures. In the case of weathering along fractures, such as in the grains 2000237ilm2 (Fig. 26) and 2000256ilm1 (Fig. 28), there appears to be a high degree of symmetry in the composition of the alteration material on either side of the fracture. The fact that alteration along fractures is a widespread phenomenon suggests that the alteration took place at low temperature, and did not occur during retrograde metamorphism. The alteration therefore most likely takes place in situ. It is not possible to determine if the alteration of ilmenite took place only at or close to outcrop surface, but from the information given in Stendal et al. (2003) it appears that most rock samples were collected in quarries or along road cuts. Also, the specimen appear fresh, and without weathered surfaces, so it is concluded that the incipient ilmenite alteration is a pervasive process that inflicts the rocks to several meters or even tens of meters below outcrop surface.

8.3 Phosphate impurities

Several altered ilmenite grains show significant concentrations of phosporous, usually > 0.2 wt. % when present. Unaltered ilmenite always shows phosphorous concentrations lower than the level of detection (0.01 wt. %), and the phosphorous must therefore have been introduced during the alteration. When phosphorous is present, it always occurs with calcium, and approximately in 1:1 proportions of P_2O_5 and CaO (Fig. 35), hence representing apatite crystals. As stated above, it is here interesting to note, that while other impurities, mostly silicates, appear to decrease in abundance during progressive leaching of a particular ilmenite grain, apatite, once formed, stays at the given concentration. It has, however, not been possible to detect any systematics in the process of phosphate introduction to the alteration process. For instance, as noted above, grain ilm3 in sample 2000232 has abundant phosphate inclusions, while ilm4 in the same sample, and which show otherwise identical alteration style, has P_2O_5 close to detection limit.

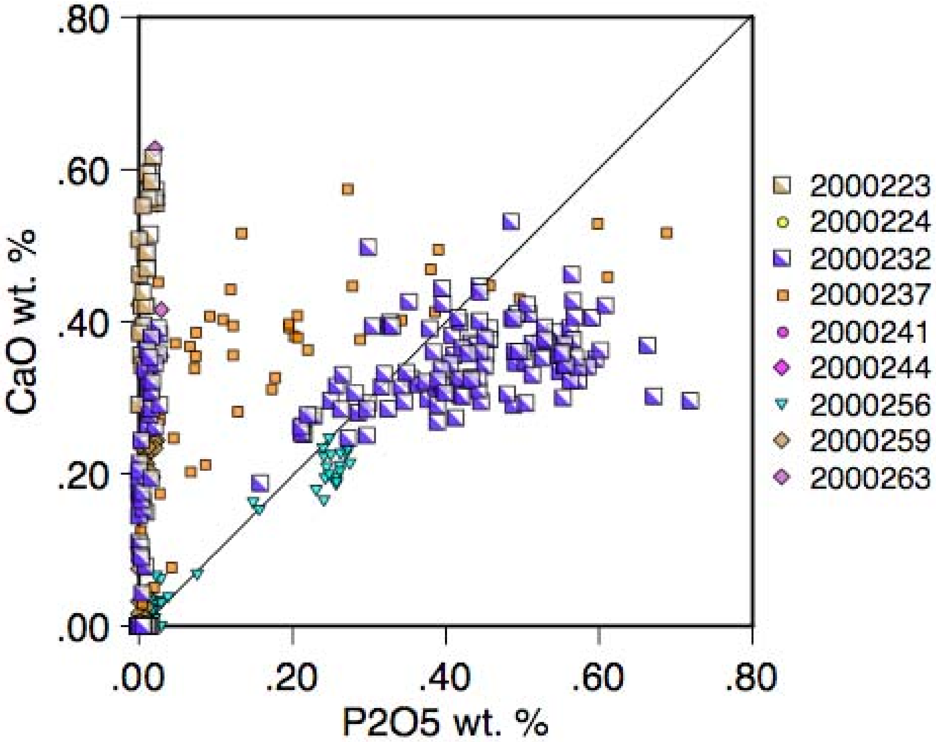

Figure 35. *Electron micro-probe data for altered ilmenite grains. Line gives 1:1 of P2O5 and CaO, which is approximately the proportions found in apatite.*

9. Concluding remarks

There are several major points to be drawn from this study. The first is that it is firmly established that the main source for the high grade ilmenite deposits along the SW Kerala State coast is the khondalite belt lithologies. More specifically, source must be found in the sillimanite-bearing, orthopyroxene-absent rocks, in which the garnets chemistry is characterized by low grossular component and low Mn. This point is further corroborated by the high modal contents of both garnet and ilmenite in these rocks. Perhaps this latter point also bears the explanation why the high grade ilmenite deposits almost exclusively contains garnets from these sillimanite-bearing rocks, as these simpley are the major source of garnet.

Another important observation is the degree of ilmenite alteration, which in some samples is relatively advanced, so that e. g. sample 2000232 contains one large, completely altered ilmenite grain, now hydroxy-pseudorutile with Ti# of 97. While such advanced alteration is found in several grains, no grains have been found to contain recrystallized rutile or anatase with nearly 100 wt. % TiO_2. One such example is found in Hough (2003), Plate 8, p. 58, which shows stubby TiO_2 crystals surrounding an unaltered ilmenite grain. One of the questions coming out from this study is whether the ilmenite alteration processes, found to be initiated already within the source rock, is of the required style to eventually produce the high grade ilmenite from Kerala State deposits. The apparent widespread occurrence of partly, and even in a few cases completely, altered ilmenite in the rock samples is surpricing because the sediment samples from rivers draining the khondalite belt shows no significant increase in TiO_2 of average ilmenite. One explanation could be that the fragile texture of the pseudo-rutile (see e. g. Fig. 20) renders it unlikely for such grains to survive erosion and transport through the drainage systems. In this way, it is mainly the unaltered ilmenite grains that make it to the sedimentary basins, where the subsequent alteration must be considerably more efficient, since the grains at this stage are liberated from the rocks and can be attacked from all surfaces and fractures. Comparing the distribution of TiO_2 in Ti minerals from the river samples 2000210 and 218 (north Kerala) with 2000231, 233, and 235 shows that the first two samples contain few grains with TiO_2 higher than the stoichiometric 52 wt. % (2000218 has a few at around 60 wt. %). The latter three samples which comes from the khondalite belt contain significant proportions of high Ti ilmenite and leucoxene (pseudo-rutile), some of which could be similar to the altered ilmenite grains documented above, perhaps cemented with clay or carbonate to make them more resistant to erosion.

10. References cited

Bernstein, S., 2003, Ilmenite heavy sand deposits, South India - provenance and christry clues to their origin: GEUS Report, v. 2003/100, p. 1-123.

Chacko, T., Ravindra Kumar, G.R., and Newton, R.C., 1987, Metamorphic P-T conditions of the Kerala (South India) khondalite belt, a granulite facies supracrustal terrain: Journal of Geology, v. 95, p. 343-358.

Frost, M.T., Grey, I.E., Harrowfield, I.R., and Mason, K., 1983, The dependence of alumina and silica contents on the extent of alteration of weathered ilmenites from western Australia: Mineralogical Magazine, v. 47, p. 201-208.

Grey, I.E., and Reid, A.F., 1975, The structure of pseudorutile and its role in the natural alteration of ilmenite: American Mineralogist, v. 60, p. 898-906.

Grey, I.E., Watts, J.A., and Bayliss, P., 1994, Mineralogical nomenclature: pseudorutile revalidated and neotype given: Mineralogical Magazine, v. 58, p. 597-600.

Hough, F.E., 2003, Summary of work on ilmenite geochemistry: Confidential report for DuPont, p. 1-77.

Nandakumar, V., and Harley, S.L., 2000, A reappraisal of the pressure-temperature path of granulites from the Kerala Khondalite Belt, Southern India: Journal of Geology, v. 108, p. 687-703.

Sabeen, H.M., Ramanujam, N., and Morton, A.C., 2002, The provenance of garnet: constraints provided by studies of coastal sediments from southern India: Sedimentary Geology, v. 152, p. 279-287.

Stendal, H., Prasad, H., and Vasudev, V.N., 2003, Heavy mineral sands in Kerala and Tamil Nadu, southern India: GEUS Report, v. 2003/13.

11. Appendix 1

Petrographic descriptions of hand specimens and thin sections, Kerala Khondalite Belt

Sample number: 2000208
Field number: K1
Rock name: Orthopyroxene gneiss (charnockite)
Rock description: Thick section. This is a very coarse-grained grey rock comprised of plagioclase (c. 80%) and large laths of brown orthopyroxene (c. 20%, 0.5 to 1 cm length). It shows no evident gneissic layering or preferred mienral orientation.

Sample number: 2000209
Field number: K2
Rock name: Garnet-clinopyroxene gneiss
Rock description: This is a fine to medium-grained garnet-clinopyroxene-plagioclase gneiss. It shows no gneissic layering or preferred orientation of minerals. It is comprised of plagioclase (c. 35%), clinopyroxene (c. 35%, probably augite), garnet (c. 25%), ilmenite (c. 5%) and rutile (c. 5%). It is difficult to determine if quartz is present given the thickness of the section. Garnet has inclusions of ilmenite and probably other phases, though it is difficult to determine what these are in such a thick section. Garnet is commonly partly rimmed by clinopyroxene ± ilmenite and rutile. Plagioclase shows extensive recrystallisation.
Some P-T path information could possibly be obtained from investigation of the garnet-clinopyroxene reaction textures.

Sample number: 2000214
Field number: K7
Rock name: Dioritic gneiss
Rock description: Thick section. This is a fine to medium-grained clinopyroxene-plagioclase gneiss, with mm-thick compositional layering defining the foliation. It is comprised of plagioclase (c. 40%, maybe a little quartz?), clinopyroxene (c. 25%), rutile (c. 15%) and fine-grained opaque phases (c. 20%). Clinopyroxene and large rutile show heavy alteration to fine-grained opaque phases, and plagioclase to a fine-grained plagioclase matrix. It is difficult to determine the nature of the fine-grained opaque phases that occur as late alteration products.

Sample number: 2000216
Field number: K10
Rock name: Horblende-biotite gneiss
Rock description: Thick section. This is a medium-grained banded biotite-plagioclase gneiss. Compositional layering on mm- to cm-scale and aligned biotite flakes define a moderate gneissic foliation. It is dominantly comprised of plagioclase (c. 40%) and

quartz (c. 25%) in granoblastic textures, with aligned biotite (c. 20%), hornblende (c. 10%), and accessory apatite (?) and browny-red to opaque phases (probably rutile and ilmenite). Large, dark grains of hornblende are difficult to recognise because of the thickness of the section, making them almost opaque.

Sample number: 2000217
Field number: K11
Rock name: Hornblende dioritic gneiss (charnockite)
Rock description: Thick section. This is a dark, coarse-grained granoblastic gneiss, dominantly comprised of granoblastic coarse-grained plagioclase (c. 60%), clinopyroxene (probably augite, c. 10%), brown amphibole (c. 15%), minor orthopyroxene (c. 10%), biotite (c. 5%), and accessory ilmenite. Ilmenite, plagioclase, amphibole, clino- and orthopyroxene are intergrown in equilibrated textures. Clinopyroxene has some inclusions of ilmenite and commonly shows partial to heavy alteration to fine-grained hornblende (?).

Sample number: 2000221
Field number: K16
Rock name: Hornblende dioritic gneiss (?)
Rock description: Thick section. This is a medium to coarse-grained granoblastic rock with a grey-green greasy appearance. It is dominated by plagioclase (c. 60%), brown amphibole (c. 25%), lesser quartz-K-feldspar (? c. 10%) and biotite (c. 5%) and possibly some accessory opaque phases (difficult to tell these apart from biotite in some cases in such a thick section).

Sample number: 2000222
Field number: K19
Rock name: Hornblende dioritic gneiss
Rock description: Thick section. Medium to coarse-grained granoblastic plagioclase-rich gniess. Mm to cm thick amphibole-biotite-rich and plagioclase-rich compositional layers define a moderate gneissic fabric. Foliation is also defined by aligned biotite flakes. Within a amphibole -biotite-rich layer the rock is comprised of plagioclase (c. 40%), brown amphibole (c. 40%), biotite (c. 15%), and accessory ilmenite and tourmaline. All phases are intergrown in equilibrated textures. Ilmenite forms discrete grains, but also typically occurs at grain intersections and along grain boundaries and is therefore formed, at least in part, at a late-stage.

Sample number: 2000223
Field number: K20
Rock name: Two-pyroxene gabbroic gneiss (charnockite)
Rock description: Fine-grained granoblastic gabbro, comprising plagioclase (c. 60%), clinopyroxene (probably augite, c. 20%), orthopyroxene (c. 10%), biotite (c. 10%) and accessory opaque phases (ilmenite?). All phases in equilibrated textures.
Temperature estimates from two-pyroxene thermometry

Sample number: 2000224

Field number: K23

Rock name: Granodioritic gneiss

Rock description: Thick section. Fine to medium-grained biotite-bearing granodioritic gneiss with patchy occurrences of deep-red staining (not garnet). A gneissic fabric is defined by discontinuous mm to cm-scale compositional layering of biotite-rich and plagioclase-rich layers. The rock is comprised of quartz (c. 40%), plagioclase (c. 30%), K-feldspar (?, c. 10%), opaque phases (c. 15%), and biotite (c. 5%). One of the opaque phases (possibly magnetite) shows partial alteration to a second, high-reflectivity opaque phase (probably ilmenite). Patchy deep-red staining is thought to be an Fe-staining alteration effect on K-feldspar where this is proximal to magnetite (?).

Sample number: 2000232

Field number: K31

Rock name: Garnetiferous quartzo-feldspathic gneiss

Rock description: Thick section. Coarse-grained garnet-porphyroblastic gneiss with a weak gneissic fabric defined by compositional layering of more biotite-rich and plagioclase-rich layers, and aligned biotite flakes. Porphyroblastic pinky-red garnet (0.2 to 1 cm) contains abundant inclusions of biotite, quartz, ilmenite, and hematite (?). The cores of the garnet porphyroblasts appear to be, at least in part, wrapped by fine-grained abundant aligned laths of sillimanite, which in turn are overgrown by garnet. These sillimanite defined a foliation, which appears to be the same as the gneissic fabric (though it is difficult to determine exactly because I am not sure where the thin section comes from in relation to the hand specimen). There appears to be no sillimanite in the medium-coarse-grained matrix, though garnet (c. 15%) coexists with matrix plagioclase (c. 30%), quartz (c. 40%), K-feldspar (? c. 10%), biotite (c. 5%), and accessory ilmenite and hematite (?).

This rock contains an assemblage suitable for P-T work (garnet-sillimanite-plagioclase-quartz, and garnet-ilmenite). The absence of sillimanite in the matrix assemblage, compared to its presence in the garnet inclusion assemblage may be useful in determining a P-T path.

Sample number: 2000234

Field number: K33

Rock name: Garnetiferous quartzo-feldspathic gneiss

Rock description: Thick section. Medium to coarse-grained garnetiferous quartzo-feldspathic gneiss. The rock has a granoblastic fabric with no obvious gneissic layering, but a weak alignment of biotite flakes. Porphyroblastic pinky-red garnet (c. 15%, 0.1 to 1 cm) contain inclusions of biotite, quartz, sillimanite and ilmenite with no obvious preferred orientation. The matrix is comprised of quartz (c. 45%), plagioclase (c. 25%), K-feldspar (?), biotite (c. 15%), and accessory ilmenite and hematite (?).

This rock contains an assemblage suitable for P-T work (garnet-sillimanite-plagioclase-quartz, and garnet-ilmenite). The absence of sillimanite in the matrix assemblage, compared to its presence in the garnet inclusion assemblage may be useful in determining a P-T path.

Sample number: 2000236
Field number: K36
Rock name: Garnetiferous quartzo-feldspathic gneiss
Rock description: Thick section. Medium-grained garnet-bearing quartzitic gneiss with a moderate gneissic fabric defined by biotite ± garnet -rich seams and mm-thick layers. The rock is dominantly comprised of quartz (c. 60%) with lesser plagioclase (c. 25%), biotite (c. 10%), and deep-red garnet (c. 5%) with accessory apatite (?) and opaque phases that may include hematite (?).

Sample number: 2000237
Field number: K37
Rock name: Garnetiferous diorite (?)
Rock description: Thick section. This is a coarse-grained plagioclase-rich (dioritic?) rock with a granoblastic texture and a weak foliation defined by aligned biotite. The rock has a greasy grey-green appearance attributed to the abundance of plagioclase (c. 60%), possibly with very fine inclusions given their brownish appearance in thin section, and lesser K-feldspar (?). The rare occurrence of myrmekite along grain boundaries is consistent with the presence of melt during peak metamorphism. Medium-grained red garnets (c. 5%) have inclusions of biotite, quartz and minor zircon and ilmenite. It is difficult to determine the proportions of quartz and K-feldspar in such a thick section, but probably these account for c. 20%. The matrix also comprises biotite (c. 10%) and accessory opaque phases (probably ilmenite ± hematite).
Temperature estimates could be made from garnet-ilmenite thermometry

Sample number: 2000241
Field number: K41
Rock name: Garnet-orthopyroxene gneiss
Rock description: Thick section. This is a sugary-textured grey-green rock. It has a granoblastic texture with no gneissosity evident. It is dominantly comprised of plagioclase (c. 35%), quartz (c. 25%, possibly including some K-feldspar), with lesser garnet (c. 15%), orthopyroxene (c. 10%), biotite (c. 10%) and accessory opaque phases (including and probably mostly ilmenite) and zircon. Garnet has abundant inclusions of quartz, biotite, and rare ilmenite and zircon.
Temperature estimates could be made from garnet-orthopyroxene and garnet-ilmenite thermometry

Sample number: 2000243
Field number: K43
Rock name: Garnetiferous granite
Rock description: This is a medium-grained white, garnet-bearing granite. It comprises quartz (c. 40%), plagioclase (c. 25%), K-feldspar (c. 25%), garnet (c. 5%) and accessory zircon and an opaque phase that is probably ilmenite. Garnet is largely inclusion-free, but does contain some small inclusions of quartz. Perthitic ternary feldspars are common and show a range of exsolution and blebby textures. They are also weakly sericitised. Quartz and K-feldspar commonly occur in myrmekitic textures.

Temperature estimates might be possible using ternary-feldspar thermometry and garnet-ilmenite thermometry.

Sample number: 2000244
Field number: K44
Rock name: Garnet-bearing granodioritic gneiss
Rock description: This is a medium to coarse-grained grey-green sugary-textured rock. It is comprised of quartz (c. 50%), plagioclase (c. 25%), K-feldspar (c. 15%), garnet (c. 5%) in granoblastic textures with accessory biotite, hematite, ilmenite and relict orthopyroxene. Garnet has some inclusions of biotite, and quartz. Relict orthopyroxene (?) is heavily altered to hematite, ilmenite, chlorite and quartz.
Temperature estimates could be made using garnet-ilmenite thermometry.

Sample number: 2000251
Field number: K51
Rock name: Garnet-bearing granodiorite
Rock description: This is a garnet-bearing quartzo-feldspathic gneiss with no obvious fabric. It is comprised of quartz (c. 40%), plagioclase (c. 25%), ternary feldspar (c. 10%, perthitic), K-feldspar (c. 10%), garnet (c. 10%), biotite (c. 5%) and accessory ilmenite, muscovite and zircon. These phases generally occur in granoblastic textures. Quartz and K-feldspar are commonly seen in myrmekitic textures. Garnet is commonly porphyroblastic and contains inclusions of biotite, quartz, ilmenite and zircon.
Temperature estimates could be made using garnet-ilmenite thermometry.

Sample number: 2000256
Field number: K56
Rock name: Garnet-orthopyroxene gneiss
Rock description: This is a pale, orange-weathered rock with a weak to moderate gneissic fabric defined by a weak compositional layering of quartzo-feldspathic and garnet-orthopyroxene-rich layers, and by alignment of elongate orthopyroxene grains. The rock is comprised of quartz (c. 40%), plagioclase (c. 20%), K-feldspar (c. 10%), minor perthitic feldspar (c. 10%), orthopyroxene (c. 10%), garnet (c. 5%) and biotite (c. 5%) with accessory ilmenite and possibly sillimanite. Garnet, orthopyroxene, ilmenite, plagioclase, K-feldspar and quartz are intergrown in equilibrated textures. Quartz and K-feldspar can be observed in myrmekitic textures in places. Biotite shows partial replacement by quartz along its margins (biotite-quartz symplectites), which may be indicative of prograde breakdown.
P-T determinations may be made with this rock via garnet-orthopyroxene and garnet-ilmenite thermometry and barometry.

Sample number: 2000257
Field number: K57
Rock name: Garnet-orthopyroxene gneiss
Rock description: This is a medium-grained grey-green rock with no obvious gneissic fabric. Biotite laths show no preferred orientation. It is comprised of quartz (c. 40%),

plagioclase (c. 25%), K-feldspar (c. 15%), ternary feldspar (c. 10%), orthopyroxene (c. 5%), biotite (c. 5%), garnet (c. 5%) and accessory ilmenite, zircon. Garnet, orthopyroxene, ilmenite, plagioclase, quartz, K-feldspar and biotite and intergrown in equilibrated textures. Garnet has inclusions of biotite and quartz and commonly shows development of fine-grained garnet-quartz symplectic overgrowths on its rims. Similarly garnet-quartz symplectites are rarely developed as partial replacement products of biotite.
P-T determinations may be made with this rock via garnet-orthopyroxene and garnet-ilmenite thermometry and barometry and the reaction textures could be investigated for P-T path determinations.

Sample number: 2000259
Field number: K61
Rock name: Two-pyroxene gneiss (charnockite)
Rock description: This is a medium-grained two-pyroxene orthogneiss. It has a homogeneous granoblastic texture with no evident gneissic layering or preferred orientation of minerals. It is comprised of plagioclase (c. 20%), orthopyroxene (c. 25%), clinopyroxene (c. 25%, probably augite), biotite (c. 15%), K-feldspar (c. 10%), and ilmenite (c. 5%). All are intergrown in equilibrated textures.
Temperature estimates may be possible from two-pyroxene thermometry.

Sample number: 2000263
Field number: K66
Rock name: Garnet-bearing granodioritic gneiss
Rock description: This is a medium to coarse-grained garnet-bearing quartzo-feldspathic rock. It shows no gneissic layering or preferred orientation of minerals. The rock is comprised of plagioclase (c. 40%), quartz (c. 30%), K-feldspar (c. 20%), biotite (c. 5%), garnet (c. 5%) and accessory ilmenite. The rock has a medium-grained granoblastic texture, though there has also been some late, fine-grained quartz regrowth, particularly along grain boundaries. The garnets have inclusions of quartz, ilmenite, biotite and K-feldspar.
Temperatures may be possible from garnet-ilmenite thermometry.

Sample number: 2000264
Field number: K67
Rock name: Garnet-bearing granodioritic gneiss
Rock description: This is a medium-grained garnet-biotite felsic gneiss with a gneissosity defined by cm scale garnet-biotite-rich and plagioclase-rich compositional layering. Biotite flakes show only a weak preferred orientation. It is comprised of quartz (c. 30%), plagioclase (c. 25%, some perthitic), K-feldspar (c. 20%), garnet (c. 10%), biotite (c. 10%), hematite (c. 3%), and accessory ilmenite, apatite and zircon. Quartz and K-feldspar are commonly seen in myrmekitic textures, consistent with the presence of melt during peak metamorphism. Porphyroblastic garnet (c. 0.1 to 0.6 cm) contain inclusions of quartz, biotite, hematite, ilmenite.
Temperature estimates may be possible from garnet-ilmenite thermometry.

12. Appendix 2

Average ilmenite and garnet compositions for the rock samples

Ilmenite

GEUS #	Field#	Al2O3	MnO	CaO	P2O5	MgO	SiO2	FeO	TiO2	Cr2O3	Nb2O5	Total
2000208	K1	.063	.280	.004	.005	1.349	.010	52.17	45.84	.045	.000	99.77
2000209	K2	.044	.163	.000		.498	.006	48.58	50.38	.017		
2000217	K11	.054	2.987	.000		.540	.003	47.31	48.86	.061		
2000221	K16	.066	.171	.000	.000	.688	.000	46.43	52.94	.028	.008	100.32
2000222	K19	.075	1.043	.000		.726	.081	49.52	47.92	.029		
2000224	K23	.046	6.294	.000	.000	1.077	.020	42.35	49.79	.016	.009	99.60
2000232	K31	.056	.161	.000	.003	.646	.022	46.13	52.79	.031	.014	99.86
2000234	K33	.046	.126	.000		1.560	.004	45.07	53.35	.062	.005	
2000236	K36	.058	.159	.005	.004	.197	.014	48.06	51.68	.011	.076	100.27
2000237	K37	.063	.246	.000	.003	.215	.017	47.25	51.58	.020	.003	99.39
2000241	K41	.049	.286	.000		.650	.004	47.48	51.63	.018		
2000243	K43	.042	.177	.000	.003	1.502	.002	45.21	53.23	.043	.000	100.20
2000244	K44	.039	.226	.000		.269	.001	49.74	49.53	.018	0.000	
2000251	K51	.047	.125	.000		.320	.002	47.29	52.48	.030	.047	
2000256	K56	.053	.280	.000	.004	.157	.016	47.42	51.32	.028	.004	99.28
2000257	K57	.054	.363	.001		.555	.009	47.25	52.14	.027		
2000259	K61	.065	.470	.002	.002	.777	.058	45.73	52.06	.041	.000	99.20
2000263	K66	.040	.150	.000	.003	.796	.133	44.63	53.03	.030	.010	98.82
2000264	K67	.051	.146	.000	.005	.754	.076	45.60	52.14	.021	.025	98.82

Garnet

GEUS #	Field#	MgO	Al2O3	SiO2	CaO	TiO2	Cr2O3	MnO	FeO	Total	Pyr	AlSpite	UGraAndite
2000208	K1												
2000209	K2	3.37	20.75	37.74	7.126	.044	.017	.760	31.00	100.80	13.37	66.45	20.18
2000217	K11												
2000221	K16												
2000222	K19												
2000224	K23												
2000232	K31	6.57	22.00	38.18	1.057	.046	.022	.548	33.18	101.60	25.64	71.40	2.96
2000234	K33	7.43	21.78	38.16	1.108	.050	.054	.484	31.63	100.70	29.00	67.89	3.11
2000236	K36	2.31	21.50	37.28	3.494	.050	.015	.722	36.20	101.57	9.22	80.74	10.03
2000237	K37	2.43	21.29	37.07	3.415	.054	.022	.987	35.60	100.88	9.78	80.37	9.86
2000241	K41	4.86	21.27	37.62	2.276	.042	.007	1.125	33.51	100.71	19.25	74.27	6.48
2000243	K43	8.92	22.48	38.99	.689	.057	.021	.526	30.21	101.94	34.06	64.05	1.89
2000244	K44	4.39	20.79	36.84	1.916	.052	.009	1.074	34.88	99.95	17.74	76.69	5.57
2000251	K51	4.76	21.00	36.92	1.471	.062	.039	.621	34.97	99.84	19.19	76.54	4.27
2000256	K56	2.04	21.31	37.21	4.608	.042	.030	1.199	34.60	101.04	8.18	78.56	13.26
2000257	K57	4.52	21.37	37.64	2.007	.043	.023	1.251	34.25	101.10	17.87	76.42	5.71
2000259	K61												
2000263	K66	6.71	22.02	37.80	1.291	.041	.023	.542	32.06	100.52	26.46	69.88	3.66
2000264	K67	4.56	21.59	37.59	2.489	.059	.059	.652	33.42	100.43	18.06	74.85	7.09